

# DIFFERENCE-OF-CONVEX ELASTIC NET FOR COMPRESSED SENSING\*

LANG YU<sup>†</sup> AND NANJING HUANG<sup>†</sup>

**Abstract.** This work proposes a novel and unified sparse recovery framework, termed the difference of convex Elastic Net (DCEN). This framework effectively balances strong sparsity promotion with solution stability, and is particularly suitable for high-dimensional variable selection involving highly correlated features. Built upon a difference-of-convex (DC) structure, DCEN employs two continuously tunable parameters to unify classical and state-of-the-art models—including Lasso, Elastic Net, Ridge, and  $\ell_1 - \alpha\ell_2$ —as special cases. Theoretically, sufficient conditions for exact and stable recovery are established under the restricted isometry property (RIP), and a closed-form expression of the DCEN regularization proximal operator is derived. Moreover, two efficient optimization algorithms are developed based on the DC algorithm (DCA) and the alternating direction method of multipliers (ADMM). Within the Kurdyka-Łojasiewicz (KL) framework, the global convergence of DCA and its linear convergence rate are rigorously established. Furthermore, DCEN is extended to image reconstruction by incorporating total variation (TV) regularization, yielding the DCEN-TV model, which is efficiently solved via the Split Bregman method. Numerical experiments demonstrate that DCEN consistently outperforms state-of-the-art methods in sparse signal recovery, high-dimensional variable selection under strong collinearity, and Magnetic Resonance Imaging (MRI) image reconstruction, achieving superior recovery accuracy and robustness.

**Key words.** sparsity, compressed sensing, nonconvex optimization, DCA, global convergence

**MSC codes.** 90C26, 65K10, 49M29

**1. Introduction.** In the compressed sensing (CS) framework [5, 10], the key challenge in recovering a sparse signal  $\mathbf{x}$  from underdetermined measurements  $\mathbf{y} = \Phi\mathbf{x}$  is choosing a suitable regularization to constrain the solution. Ideally, one minimizes the  $\ell_0$  norm, i.e.,  $\min_{\mathbf{x}} \|\mathbf{x}\|_0$  subject to  $\mathbf{y} - \Phi\mathbf{x} \in \mathcal{E}$ , where  $\mathcal{E} \subseteq \mathbb{R}^m$  models noise (with  $\mathcal{E} = \{\mathbf{0}\}$  in the noiseless case). However,  $\ell_0$  minimization is NP-hard and nonconvex. Candès et al. [5] showed that if  $\Phi$  satisfies the RIP condition,  $\ell_0$  minimization can be equivalently replaced by the convex  $\ell_1$  minimization (Basis Pursuit, BP) [8], yielding  $\min_{\mathbf{x}} \|\mathbf{x}\|_1$  subject to  $\mathbf{y} - \Phi\mathbf{x} \in \mathcal{E}$ . Yet,  $\ell_1$  is dominated by large-magnitude components, whereas  $\ell_0$  is scale-invariant, so the  $\ell_1$  approximation introduces bias and may cause suboptimal recovery, especially when  $\Phi$  has highly coherent columns [13].

Recent studies have shown that nonconvex sparsity-promoting measures can not only significantly reduce the required number of measurements, but also achieve superior recovery performance and enhanced sparsity of the solution. Popular nonconvex measures include the  $\ell_p$  quasi-norm ( $p \in (0, 1)$ ) and its variants [6, 7, 9, 38], the minimax concave penalty (MCP) [43], the capped- $\ell_1$  [45], the smoothly clipped absolute deviation (SCAD) penalty [12], the transformed  $\ell_1$  ( $T\ell_1$ ) [44], as well as nonconvex measures based on probability density functions [46]. It is worth noting that these nonconvex measures are all separable in structure, i.e., they can be decomposed into a sum of identical one-dimensional functions. While separable nonconvex measures perform well in scenarios with low mutual coherence or low dynamic range, nonseparable nonconvex measures generally exhibit superior sparse recovery performance when the sensing matrix is highly coherent or the signal possesses a high dynamic range [48].

\*Submitted to the editors DATE.

**Funding:** This work was funded by the National Natural Science Foundation of China (12171339, 12471296).

<sup>†</sup>Department of Mathematics, Sichuan University, Chengdu, 610064, China (nanjinghuang@hotmail.com; njhuang@scu.edu.cn ).

Among nonseparable measures, ratio-type nonconvex measures have attracted particular attention due to their scale invariance, which enables a closer approximation to the inherently scale-invariant  $\ell_0$  “norm” (which is not a true norm). Notably, in the one-dimensional case, these two measures coincide. Ratio-type nonconvex measures were first introduced in the work of Hoyer [16], followed by extensive studies on the  $\ell_1/\ell_2$  model [27] and its associated algorithms [2, 30, 34, 41], as well as its applications in computed tomography (CT) reconstruction [33]. Xu et al. [37] established exact recovery conditions for  $\ell_1/\ell_2$  and provided sufficient conditions for its equivalence to  $\ell_0$ . Other ratio-type measures include  $(\ell_1/\ell_2)^2$  [19] and the  $q$ -ratio sparsity measure  $(\ell_1/\ell_q)^{\frac{q}{q-1}} (1 < q \leq \infty)$  [49]. A rich body of literature has also investigated the  $\ell_1/\ell_q$  ( $q > 1$ ) model, including [17, 21, 32, 35]. Despite their advantages in approximating  $\ell_0$  and promoting sparsity, ratio-type nonconvex measures suffer from highly complex structures and strong nonconvexity. In particular, they are often not globally Lipschitz continuous and may lack coercivity. These issues render theoretical analysis and algorithm design highly challenging. Moreover, some models (e.g.,  $\ell_1/\ell_2$ ) may even tend to produce an abnormally large coefficient while suppressing other nonzero components [27].

Another important class of nonseparable nonconvex measures is difference-type. The contour of such measures are closer to those of the  $\ell_0$  norm, making them more effective in promoting sparsity. The  $\ell_{1-2}$  (e.g.,  $\ell_1 - \ell_2$ ) measure is the most representative example. It was originally proposed in [11] as a sparsity-inducing penalty for nonnegative least squares problems, and later applied to sparse recovery in [25, 40], where it demonstrated superior performance over existing measures when the sensing matrix is highly coherent. Subsequently, several other difference-type measures have been proposed and extensively studied, including  $\ell_1 - \alpha\ell_2$  [14, 24],  $\ell_1 - \beta\ell_q$  [18],  $\ell_r - \alpha\ell_1$  [47],  $\ell_q - \alpha\ell_p$  ( $p \in (1, 2)$ ) [15], and weighted  $\ell_q - \alpha\ell_p$  ( $q \in (0, 1)$ ,  $p \in [q, +\infty]$ ,  $\alpha \in [0, 1]$ ) [42]. Nevertheless, difference-type measures also exhibit inherent limitations. First, as the number of dominant components (ordered by magnitude) in the signal increases, difference-type measures may gradually become biased; for instance, the behavior of  $\ell_{1-2}$  tends to approach that of  $\ell_1$  [26]. Second, classical difference-type measures primarily focus on sparsity itself and often fail to effectively capture the grouping effect when dealing with highly correlated variables, which may result in unstable solutions in practical applications.

To overcome the aforementioned limitations in balancing sparsity promotion and robustness under coherent sensing matrices, this work, inspired by Elastic Net [50], proposes a more general difference-type nonseparable sparsity measure for sparse signal recovery and high-dimensional variable selection. Specifically, we consider the following constrained optimization problem

$$(1.1) \quad \min_{\mathbf{x} \in \mathbb{R}^n} \gamma(\|\mathbf{x}\|_1 - \alpha\|\mathbf{x}\|_2) + (1 - \gamma)\|\mathbf{x}\|_2^2 \quad \text{s.t.} \quad \mathbf{A}\mathbf{x} = \mathbf{b},$$

and its unconstrained regularized form

$$(1.2) \quad \min_{\mathbf{x} \in \mathbb{R}^n} \frac{1}{2}\|\mathbf{A}\mathbf{x} - \mathbf{b}\|_2^2 + \lambda(\gamma(\|\mathbf{x}\|_1 - \alpha\|\mathbf{x}\|_2) + (1 - \gamma)\|\mathbf{x}\|_2^2),$$

where  $\mathbf{A} \in \mathbb{R}^{m \times n}$  denotes the sensing matrix,  $\mathbf{b} \in \mathbb{R}^m$  is the observation vector, and  $\mathbf{x} \in \mathbb{R}^n$  is the signal to be recovered. The parameter  $\lambda > 0$  balances the data fidelity term and the regularization term. Two key tuning parameters are introduced:  $\gamma \in (0, 1)$  controls the mixing ratio between the  $\ell_1 - \alpha\ell_2$  and  $\ell_2^2$  components, while  $\alpha \in (0, 1)$  adjusts the strength of the nonconvex difference term. The unconstrained

regularized problem (1.2) is referred to as DCEN, and the constrained problem (1.1) as CDCEN. We primarily investigate the theoretical properties of CDCEN and the optimization methods for solving DCEN. DCEN aims to combine the high-precision recovery capability of nonconvex regularization with the stability of Elastic Net, and seeks an optimal balance between sparsity induction and bias control through adjustable parameters. Notably, DCEN provides a highly unified mathematical framework: by flexibly tuning  $\gamma$  and  $\alpha$ , DCEN reduces to several classical convex and nonconvex regularization models:

- $\ell_1 - \ell_2$  model: when  $\gamma \rightarrow 1$  and  $\alpha \rightarrow 1$ , the regularization term degenerates to the difference measure  $\|\mathbf{x}\|_1 - \|\mathbf{x}\|_2$ ;
- $\ell_1 - \alpha\ell_2$  model: when  $\gamma \rightarrow 1$  and  $\alpha \in (0, 1)$ , DCEN recovers the classical nonconvex  $\ell_1 - \alpha\ell_2$  measure;
- LASSO model: when  $\gamma \rightarrow 1$  and  $\alpha \rightarrow 0$ , the  $\ell_2$  term vanishes, yielding the standard  $\ell_1$  minimization problem;
- Elastic Net model: when  $\gamma \in (0, 1)$  and  $\alpha \rightarrow 0$ , the nonconvex subtraction term disappears, reducing DCEN to Elastic Net;
- Ridge regression: when  $\gamma \rightarrow 0$  and  $\alpha \rightarrow 0$ , only the  $\ell_2^2$  term remains.

In summary, DCEN inherits the advantages of nonconvex measures in sparse approximation while retaining the ability of the Elastic Net to handle correlated variables. Compared with ratio-type measures, DCEN is constructed within the DC framework, which guarantees coercivity of the objective function and enables efficient optimization via DC algorithms (DCA). Figure 1 shows that the objective function of (1.1), by tuning the parameter  $\gamma$ , can preserve its sparsity-promoting property while effectively reducing nonconvexity and enhancing smoothness. The main contributions of this work can be summarized as follows:

- (i) Both constrained and unconstrained DCEN models are proposed and some conditions are obtained for ensuring the exact and stable recovery based on RIP, which extends and improves the existing results in [40, 39].
- (ii) A closed-form analytical solution of the proximal operator is derived for DCEN regularization under some mild assumptions, and further an efficient DC decomposition and a variable-splitting strategy are, respectively, developed for solving DCEN, which lead to DCA- and ADMM-based iteration schemes.
- (iii) Global convergence and linear convergence rates of the proposed DCA and ADMM are rigorously established under the KL framework, which extend the convergence result of DCA proposed in [40].
- (iv) DCEN is extended to structured inverse problems by incorporating total variation regularization to form the DCEN-TV model, and an efficient algorithm based on the split Bregman method is developed, demonstrating its extensibility in image-related tasks.
- (v) Systematic experiments are provided for noiseless or noisy signal recovery, high-dimensional correlated variable selection, and MRI reconstruction to show that the performance of DCEN consistently is superior to the state-of-the-art methods in terms of both accuracy and stability.

**2. Recovery properties of CDCEN.** This section systematically analyzes the theoretical properties of CDCEN with respect to exact recovery and robust recovery.

**2.1. Exact and stable recovery.** We first show the following lemmas concerning the measure  $\|\mathbf{x}\|_1 - \alpha\|\mathbf{x}\|_2$ , which will be frequently invoked later in the proofs.

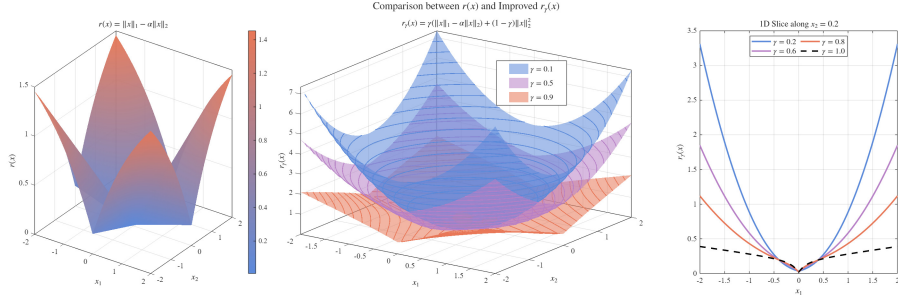


Fig. 1: Geometric comparison of  $r(\mathbf{x}) = \|\mathbf{x}\|_1 - \alpha \|\mathbf{x}\|_2$  and its variant  $r_\gamma(\mathbf{x}) = \gamma(\|\mathbf{x}\|_1 - \alpha \|\mathbf{x}\|_2) + (1 - \gamma) \|\mathbf{x}\|_2^2$ .

LEMMA 2.1. Let  $\alpha \in (0, 1)$  and  $\mathbf{x} \in \mathbb{R}^n \setminus \{\mathbf{0}\}$  with  $\|\mathbf{x}\|_0 = s$  and  $\Lambda = \text{supp}(\mathbf{x})$ . Then the following statements hold:

$$(a) (n - \alpha\sqrt{n})x_{\min} + (1 - \alpha)(\|\mathbf{x}\|_1 - nx_{\min}) \leq \|\mathbf{x}\|_1 - \alpha \|\mathbf{x}\|_2 \leq (\sqrt{n} - \alpha)\|\mathbf{x}\|_2,$$

$$(b) (s - \alpha\sqrt{s})x_{\min} + (1 - \alpha)(\|\mathbf{x}_\Lambda\|_1 - sx_{\min}) \leq \|\mathbf{x}_\Lambda\|_1 - \alpha \|\mathbf{x}_\Lambda\|_2 \leq (\sqrt{s} - \alpha)\|\mathbf{x}\|_2,$$

where  $x_{\min}$  in (a) is defined as  $x_{\min} = \min_j |x_j|$  and  $x_{\min}$  in (b) is defined as  $x_{\min} = \min_{j \in \Lambda} |x_j|$ .

*Proof.* (a) By the Cauchy–Schwarz inequality  $\|\mathbf{x}\|_1 \leq \sqrt{n}\|\mathbf{x}\|_2$ , it follows that  $\|\mathbf{x}\|_1 - \alpha \|\mathbf{x}\|_2 \leq \sqrt{n}\|\mathbf{x}\|_2 - \alpha \|\mathbf{x}\|_2 = (\sqrt{n} - \alpha)\|\mathbf{x}\|_2$ .

Next, we establish the lower bound. Without loss of generality, assume  $|x_1| \geq |x_2| \geq \dots \geq |x_n|$ . We define the residual term of the  $\ell_1$ -norm as  $\Delta_1 = \|\mathbf{x}\|_1 - n \cdot x_{\min} = \sum_{i=1}^n |x_i| - \sum_{i=1}^n x_{\min} = \sum_i^n (|x_i| - x_{\min})$ . Since for any  $i \in \{1, 2, \dots, n\}$ , we have  $|x_i| \geq x_{\min}$  and  $\Delta_1 \geq 0$ . Moreover,  $\Delta_1 = 0$  if and only if all nonzero elements  $|x_i|$  are equal to  $x_{\min}$ . Hence, the  $\ell_1$ -norm can be written as

$$(2.1) \quad \|\mathbf{x}\|_1 = n \cdot x_{\min} + \Delta_1.$$

Let  $\delta_i = |x_i| - x_{\min} \geq 0$ . Then we have  $\Delta_1 = \sum_{i=1}^n \delta_i$  and

$$(2.2) \quad \begin{aligned} \|\mathbf{x}\|_2^2 &= \sum_{i=1}^n |x_i|^2 = \sum_{i=1}^n (x_{\min} + \delta_i)^2 = \sum_{i=1}^n (x_{\min}^2 + 2x_{\min}\delta_i + \delta_i^2) \\ &= n \cdot x_{\min}^2 + 2x_{\min} \sum_{i=1}^n \delta_i + \sum_{i=1}^n \delta_i^2 = n \cdot x_{\min}^2 + 2x_{\min}\Delta_1 + \|\boldsymbol{\delta}\|_2^2. \end{aligned}$$

From the inequality  $\|\boldsymbol{\delta}\|_2 \leq \|\boldsymbol{\delta}\|_1$ , one has

$$(2.3) \quad \|\boldsymbol{\delta}\|_2^2 = \sum \delta_i^2 \leq \left( \sum \delta_i \right)^2 = \Delta_1^2.$$

Substituting (2.3) into the expression of  $\|\mathbf{x}\|_2^2$  in (2.2) leads to  $\|\mathbf{x}\|_2^2 \leq n \cdot x_{\min}^2 + 2x_{\min}\Delta_1 + \Delta_1^2$ . Note that  $(\sqrt{n}x_{\min} + \Delta_1)^2 = nx_{\min}^2 + 2\sqrt{n}x_{\min}\Delta_1 + \Delta_1^2$ . Since  $n \geq 1$  (the number of entries in  $\mathbf{x}$  is at least one), it follows that  $\sqrt{n} \geq 1$ . By the fact that  $x_{\min} \geq 0$  and  $\Delta_1 \geq 0$ , we have  $2x_{\min}\Delta_1 \leq 2\sqrt{n}x_{\min}\Delta_1$  and  $nx_{\min}^2 + 2x_{\min}\Delta_1 + \Delta_1^2 \leq nx_{\min}^2 + 2\sqrt{n}x_{\min}\Delta_1 + \Delta_1^2 = (\sqrt{n}x_{\min} + \Delta_1)^2$ . Taking the square root on both sides gives  $\sqrt{nx_{\min}^2 + 2x_{\min}\Delta_1 + \Delta_1^2} \leq \sqrt{n}x_{\min} + \Delta_1$ . Combining with  $\|\mathbf{x}\|_2^2 \leq nx_{\min}^2 + 2x_{\min}\Delta_1 + \Delta_1^2$ , the upper bound of  $\|\mathbf{x}\|_2$  is given by  $\|\mathbf{x}\|_2 \leq \sqrt{n}x_{\min} + \Delta_1$ . Substituting

the expression of  $\|\mathbf{x}\|_1$  in (2.1) and the upper bound of  $\|\mathbf{x}\|_2$  into  $\|\mathbf{x}\|_1 - \alpha\|\mathbf{x}\|_2$ , we have

$$(2.4) \quad \|\mathbf{x}\|_1 - \alpha\|\mathbf{x}\|_2 \geq \|\mathbf{x}\|_1 - \alpha(\sqrt{n}x_{\min} + \Delta_1).$$

Since  $\Delta_1 = \|\mathbf{x}\|_1 - nx_{\min}$ , it follows from (2.4) that

$$(2.5) \quad \|\mathbf{x}\|_1 - \alpha\|\mathbf{x}\|_2 \geq (n - \alpha\sqrt{n})x_{\min} + (1 - \alpha)(\|\mathbf{x}\|_1 - nx_{\min}).$$

(b) It is worth noting that  $\|\mathbf{x}\|_1 - \alpha\|\mathbf{x}\|_2$  depends only on the nonzero components of  $\mathbf{x}$ , that is,  $\|\mathbf{x}\|_1 - \alpha\|\mathbf{x}\|_2 = \|\mathbf{x}_\Lambda\|_1 - \alpha\|\mathbf{x}_\Lambda\|_2$ . Hence, statement (b) directly follows by applying (a) to  $\mathbf{x}_\Lambda$ .  $\square$

*Remark 2.2.* The newly derived lower bound is sharper than  $(n - \alpha\sqrt{n})x_{\min}$  in [40]. Since  $\|\mathbf{x}\|_1 - nx_{\min} = \Delta_1 \geq 0$  and  $1 - \alpha \geq 0$ , the new bound becomes strictly greater than  $(n - \alpha\sqrt{n})x_{\min}$  whenever the vector  $\mathbf{x}$  is not flat (i.e.,  $\|\mathbf{x}\|_1 > nx_{\min}$ ). The proposed bound explicitly exploits the residual term  $\Delta_1$ , which measures the excess of the  $\ell_1$ -norm over its minimum value  $nx_{\min}$ , thus providing a sharper estimation.

**LEMMA 2.3.** *Let  $\alpha \in (0, 1)$  and  $\mathbf{x} \in \mathbb{R}^n \setminus \{\mathbf{0}\}$  with  $\|\mathbf{x}\|_0 = s$  and  $\Lambda = \text{supp}(\mathbf{x})$ . Assume that there exist constants  $C \geq 1$  and  $p \geq 0$  such that  $|x_i| \geq Ci^{-p} \min_j |x_j|$  for all  $i \in \{1, 2, \dots, n\}$ . Then, the following statements hold:*

$$(a) Cx_{\min} \left( \alpha n^{\frac{1}{2}-p} \left( n^{\frac{1}{2}} - 1 \right) + (1 - \alpha)H_{n,p} \right) \leq \|\mathbf{x}\|_1 - \alpha\|\mathbf{x}\|_2,$$

$$(b) Cx_{\min} \left( \alpha s^{\frac{1}{2}-p} \left( s^{\frac{1}{2}} - 1 \right) + (1 - \alpha)H_{s,p} \right) \leq \|\mathbf{x}_\Lambda\|_1 - \alpha\|\mathbf{x}_\Lambda\|_2,$$

where  $x_{\min}$  is defined as the one in Lemma 2.1 and  $H_{n,p} = \sum_{i=1}^n i^{-p}$ .

*Proof.* (a) Without loss of generality, assume that  $|x_1| \geq |x_2| \geq \dots \geq |x_n|$ , and let  $\min\{|x_i|\} = x_{\min}$ . According to the assumption, we have  $|x_i| \geq Ci^{-p}x_{\min}$  and so

$$(2.6) \quad \|\mathbf{x}\|_1 = \sum_{i=1}^n |x_i| \geq \sum_{i=1}^n Ci^{-p}x_{\min} = Cx_{\min} \sum_{i=1}^n i^{-p}.$$

Let  $H_{n,p} = \sum_{i=1}^n i^{-p}$ . Then  $\|\mathbf{x}\|_1 \geq Cx_{\min}H_{n,p}$ . By Lemma 2.1, substituting (2.6) into (2.5) yields  $\|\mathbf{x}\|_1 - \alpha\|\mathbf{x}\|_2 \geq (\alpha n - \alpha\sqrt{n})x_{\min} + (1 - \alpha)Cx_{\min}H_{n,p}$ . It follows from  $x_{\min} \geq Cn^{-p}x_{\min}$  that  $(\alpha n - \alpha\sqrt{n})x_{\min} + (1 - \alpha)Cx_{\min}H_{n,p} \geq Cx_{\min}(\alpha n^{\frac{1}{2}-p}(n^{\frac{1}{2}} - 1) + (1 - \alpha)H_{n,p})$ .

(b) Statement (b) directly follows by applying (a) to  $\mathbf{x}_\Lambda$ .  $\square$

*Remark 2.4.* In Lemma 2.3, if the parameters  $C$  and  $p$  are properly chosen, the new lower bound  $Cx_{\min} \left( \alpha s^{\frac{1}{2}-p} \left( s^{\frac{1}{2}} - 1 \right) + (1 - \alpha)H_{s,p} \right)$  becomes tighter than the bound  $(s - \alpha\sqrt{s})x_{\min}$ . For  $C = s^p$  with  $p \geq 0$ , one has  $Cx_{\min} \left( \alpha s^{\frac{1}{2}-p} \left( s^{\frac{1}{2}} - 1 \right) + (1 - \alpha)H_{s,p} \right) = x_{\min} \left( \alpha(s - \sqrt{s}) + (1 - \alpha)s^pH_{s,p} \right)$ . Letting  $\Delta L = x_{\min} \left( \alpha(s - \sqrt{s}) + (1 - \alpha)s^pH_{s,p} \right) - (s - \alpha\sqrt{s})x_{\min}$ , we have  $\Delta L = (\alpha s - s + (1 - \alpha)s^pH_{s,p})x_{\min} = (1 - \alpha)(s^pH_{s,p} - s)x_{\min}$ . If  $0 < \alpha < 1$  and  $p = 0$ , then  $s^pH_{s,0} = H_{s,0} = \sum_{i \in \Lambda} \left( \frac{s}{i} \right)^0 = s$  and  $\Delta L = 0$ . If  $0 < \alpha < 1$  and  $p > 0$ , then for any  $i \in \{1, 2, \dots, s-1\}$ , it holds that  $s/i > 1$  and  $(s/i)^p > 1$ . Thus, for any  $s \geq 2$ , one has

$$(2.7) \quad \sum_{i \in \Lambda} \left( \frac{s}{i} \right)^p = \left( \frac{s}{1} \right)^p + \dots + \left( \frac{s}{s-1} \right)^p + \left( \frac{s}{s} \right)^p > s.$$

The summation in (2.7) includes  $s$  terms, each greater than or equal to 1, with at least  $s-1$  terms strictly greater than 1. Hence,  $s^pH_{s,p} = s^p \sum_{i \in \Lambda} i^{-p} = \sum_{i \in \Lambda} \left( \frac{s}{i} \right)^p > s$ . It follows that  $s^pH_{s,p} - s > 0$  and so  $\Delta L > 0$ .

LEMMA 2.5. Let  $\alpha \in (0, 1)$ ,  $\gamma \in (0, 1)$ ,  $\mathbf{x} \in \mathbb{R}^n \setminus \{\mathbf{0}\}$  with  $\|\mathbf{x}\|_0 = s$  and support  $\Lambda = \text{supp}(\mathbf{x})$ . If there exist constants  $C \geq 1$  and  $p \geq 0$  such that  $|x_i| \geq C i^{-p} \min_j |x_j|$  for all  $i \in \{1, 2, \dots, n\}$ , then the following statements hold:

(a) If  $C = n^p$  and  $p \geq 0$ , then

$$(2.8) \quad \begin{aligned} \gamma(\alpha n - \alpha\sqrt{n} + (1 - \alpha)n^p H_{n,p})x_{\min} + (1 - \gamma)\|\mathbf{x}\|_2^2 &\leq f_{\alpha,\gamma}(\mathbf{x}) \\ &\leq \gamma(\sqrt{n} - \alpha)\|\mathbf{x}\|_2 + (1 - \gamma)\|\mathbf{x}\|_2^2. \end{aligned}$$

(b) If  $\mathbf{x}$  has sparsity  $s$  and  $C = s^p$  with  $p \geq 0$ , then

$$(2.9) \quad \begin{aligned} \gamma(\alpha s - \alpha\sqrt{s} + (1 - \alpha)s^p H_{s,p})x_{\min} + (1 - \gamma)\|\mathbf{x}\|_2^2 &\leq f_{\alpha,\gamma}(\mathbf{x}) \\ &\leq \gamma(\sqrt{s} - \alpha)\|\mathbf{x}\|_2 + (1 - \gamma)\|\mathbf{x}\|_2^2. \end{aligned}$$

(c) If  $\mathbf{x}$  has sparsity  $s$  and  $\|\mathbf{x}\|_2 = r$ , then  $f_{\alpha,\gamma}(\mathbf{x}) > 0$  and  $f_{\alpha,\gamma}(\mathbf{x})$  attains its minimum when  $s = 1$ .

*Proof.* It follows from  $\alpha, \gamma \in (0, 1)$  that the statements (a) and (b) can be readily verified from Lemma 2.3. We now prove the statement (c). Since  $\alpha \in (0, 1)$  and  $\gamma \in (0, 1)$ , it follows that  $s - \alpha\sqrt{s} \geq 0$  and so  $f_{\alpha,\gamma}(\mathbf{x}) \geq \gamma(s - \alpha\sqrt{s})x_{\min} + (1 - \gamma)\|\mathbf{x}\|_2^2 > 0$ , which shows that  $f_{\alpha,\gamma}(\mathbf{x}) > 0$  for all  $\mathbf{x} \neq 0$ . Since  $\|\mathbf{x}\|_2 = r$ , one has  $f_{\alpha,\gamma}(\mathbf{x}) = \gamma\|\mathbf{x}\|_1 - \gamma\alpha r + (1 - \gamma)r^2 = \gamma(\|\mathbf{x}\|_1 - \alpha r) + (1 - \gamma)r^2$  and so the minimum of  $\|\mathbf{x}\|_1$  is achieved when the support size satisfies  $|\text{supp}(\mathbf{x})| = s = 1$ . In this case, the vector  $\mathbf{x}$  has only one nonzero entry of magnitude  $r$ , so  $\|\mathbf{x}\|_1 = r$ . Hence,  $f_{\alpha,\gamma}(\mathbf{x})$  attains its minimum when  $s = 1$ .  $\square$

Building upon the RIP-based analysis framework in [40, 4], which established sufficient conditions for the exact recovery of the  $\ell_1 - \ell_2$  minimization and BP problem, we extend such a framework to CDCEN under the distinct condition.

THEOREM 2.6. Let  $\alpha \in (0, 1)$ ,  $\gamma \in (0, 1)$ , and  $p \geq 0$ . Suppose that all the assumptions of Lemma 2.3 hold with  $C = (3s)^p$ . Let  $\bar{\mathbf{x}} \in \mathbb{R}^n \setminus \{\mathbf{0}\}$  be an  $s$ -sparse signal, i.e.,  $\|\bar{\mathbf{x}}\|_0 = s$  and  $\|\bar{\mathbf{x}}\|_2 \leq M (M > 0)$ , such that

$$a(s, \gamma, \alpha, p) = \left( \frac{\gamma(\alpha\sqrt{3s} - \alpha + (1 - \alpha)(3s)^p H_{3s,p}/\sqrt{3s})}{\gamma\sqrt{s} + \gamma\alpha + 2(1 - \gamma)M} \right)^2 > 1.$$

If the sensing matrix  $\mathbf{A}$  satisfies the RIP condition  $\delta_{3s} + a(s, \gamma, \alpha, p) \delta_{4s} < a(s, \gamma, \alpha, p) - 1$  and  $\mathbf{A}\bar{\mathbf{x}} = \mathbf{b}$ , then  $\bar{\mathbf{x}}$  is a unique solution to the optimization problem (1.1).

*Proof.* Let  $\mathbf{x}$  be any feasible solution of (1.1) satisfying the linear constraint  $\mathbf{A}\mathbf{x} = \mathbf{b}$  and has a smaller or equal function value, i.e.,  $\gamma(\|\mathbf{x}\|_1 - \alpha\|\mathbf{x}\|_2) + (1 - \gamma)\|\mathbf{x}\|_2^2 \leq \gamma(\|\bar{\mathbf{x}}\|_1 - \alpha\|\bar{\mathbf{x}}\|_2) + (1 - \gamma)\|\bar{\mathbf{x}}\|_2^2$ . Decomposing  $\mathbf{x}$  as  $\mathbf{x} = \bar{\mathbf{x}} + \mathbf{h}$  with  $\mathbf{h} \in \ker(\mathbf{A})$ , we show that  $\mathbf{h} = \mathbf{0}$ . To this end, let  $\Lambda = \text{supp}(\bar{\mathbf{x}})$  denote the support set of  $\bar{\mathbf{x}}$ , and decompose  $\mathbf{h}$  into  $\mathbf{h} = \mathbf{h}_\Lambda + \mathbf{h}_{\Lambda^c}$ , where  $\Lambda^c$  denotes the complement of  $\Lambda$ . Then

$$(2.10) \quad \gamma(\|\mathbf{x}\|_1 - \alpha\|\mathbf{x}\|_2) + (1 - \gamma)\|\mathbf{x}\|_2^2 \leq \gamma(\|\bar{\mathbf{x}}\|_1 - \alpha\|\bar{\mathbf{x}}\|_2) + (1 - \gamma)\|\bar{\mathbf{x}}\|_2^2.$$

For the  $\ell_1$ -norm term  $\|\bar{\mathbf{x}} + \mathbf{h}_\Lambda + \mathbf{h}_{\Lambda^c}\|_1$ , one has

$$(2.11) \quad \|\bar{\mathbf{x}} + \mathbf{h}_\Lambda + \mathbf{h}_{\Lambda^c}\|_1 = \|\bar{\mathbf{x}} + \mathbf{h}_\Lambda\|_1 + \|\mathbf{h}_{\Lambda^c}\|_1 \geq \|\bar{\mathbf{x}}\|_1 - \|\mathbf{h}_\Lambda\|_1 + \|\mathbf{h}_{\Lambda^c}\|_1.$$

Since  $\alpha \in (0, 1)$ , the  $\ell_2$ -norm term  $\alpha\|\bar{\mathbf{x}} + \mathbf{h}_\Lambda + \mathbf{h}_{\Lambda^c}\|_2$  satisfies

$$(2.12) \quad \alpha\|\bar{\mathbf{x}} + \mathbf{h}_\Lambda + \mathbf{h}_{\Lambda^c}\|_2 \leq \alpha(\|\bar{\mathbf{x}}\|_2 + \|\mathbf{h}_\Lambda\|_2 + \|\mathbf{h}_{\Lambda^c}\|_2).$$

Moreover,

$$(2.13) \quad (1 - \gamma) \|\bar{\mathbf{x}} + \mathbf{h}_\Lambda + \mathbf{h}_{\Lambda^c}\|_2^2 = (1 - \gamma)(\|\bar{\mathbf{x}} + \mathbf{h}_\Lambda\|_2^2 + \|\mathbf{h}_{\Lambda^c}\|_2^2).$$

Substituting (2.11), (2.12), and (2.13) into the inequality (2.10) yields

$$(2.14) \quad \begin{aligned} & \gamma(\|\bar{\mathbf{x}} + \mathbf{h}_\Lambda + \mathbf{h}_{\Lambda^c}\|_1 - \alpha\|\bar{\mathbf{x}} + \mathbf{h}_\Lambda + \mathbf{h}_{\Lambda^c}\|_2) + (1 - \gamma)\|\bar{\mathbf{x}} + \mathbf{h}_\Lambda + \mathbf{h}_{\Lambda^c}\|_2^2 \\ & \geq \gamma[\|\bar{\mathbf{x}}\|_1 - \|\mathbf{h}_\Lambda\|_1 + \|\mathbf{h}_{\Lambda^c}\|_1 - \alpha(\|\bar{\mathbf{x}}\|_2 + \|\mathbf{h}_\Lambda\|_2 + \|\mathbf{h}_{\Lambda^c}\|_2)] \\ & \quad + (1 - \gamma)(\|\bar{\mathbf{x}} + \mathbf{h}_\Lambda\|_2^2 + \|\mathbf{h}_{\Lambda^c}\|_2^2). \end{aligned}$$

It follows from (2.14) that  $\gamma[\|\bar{\mathbf{x}}\|_1 - \|\mathbf{h}_\Lambda\|_1 + \|\mathbf{h}_{\Lambda^c}\|_1 - \alpha(\|\bar{\mathbf{x}}\|_2 + \|\mathbf{h}_\Lambda\|_2 + \|\mathbf{h}_{\Lambda^c}\|_2)] + (1 - \gamma)(\|\bar{\mathbf{x}} + \mathbf{h}_\Lambda\|_2^2 + \|\mathbf{h}_{\Lambda^c}\|_2^2) \leq \gamma(\|\bar{\mathbf{x}}\|_1 - \alpha\|\bar{\mathbf{x}}\|_2) + (1 - \gamma)\|\bar{\mathbf{x}}\|_2^2$ . Simplifying and rearranging yields  $\gamma[-\|\mathbf{h}_\Lambda\|_1 + \|\mathbf{h}_{\Lambda^c}\|_1 - \alpha(\|\mathbf{h}_\Lambda\|_2 + \|\mathbf{h}_{\Lambda^c}\|_2)] + (1 - \gamma)(\|\bar{\mathbf{x}} + \mathbf{h}_\Lambda\|_2^2 + \|\mathbf{h}_{\Lambda^c}\|_2^2) \leq (1 - \gamma)\|\bar{\mathbf{x}}\|_2^2$ . By the Cauchy-Schwarz inequality, we have  $\|\bar{\mathbf{x}} + \mathbf{h}_\Lambda\|_2^2 \geq (\|\bar{\mathbf{x}}\|_2 - \|\mathbf{h}_\Lambda\|_2)^2$  and so

$$(2.15) \quad \begin{aligned} & \gamma[-\|\mathbf{h}_\Lambda\|_1 + \|\mathbf{h}_{\Lambda^c}\|_1 - \alpha(\|\mathbf{h}_\Lambda\|_2 + \|\mathbf{h}_{\Lambda^c}\|_2)] + (1 - \gamma)(\|\bar{\mathbf{x}} + \mathbf{h}_\Lambda\|_2^2 + \|\mathbf{h}_{\Lambda^c}\|_2^2) \\ & \geq \gamma[-\|\mathbf{h}_\Lambda\|_1 + \|\mathbf{h}_{\Lambda^c}\|_1 - \alpha(\|\mathbf{h}_\Lambda\|_2 + \|\mathbf{h}_{\Lambda^c}\|_2)] \\ & \quad + (1 - \gamma)(\|\bar{\mathbf{x}}\|_2^2 + \|\mathbf{h}_{\Lambda^c}\|_2^2 - 2\|\bar{\mathbf{x}}\|_2\|\mathbf{h}_{\Lambda^c}\|_2). \end{aligned}$$

Simplifying and rearranging yields  $\gamma\|\mathbf{h}_{\Lambda^c}\|_1 - \gamma\alpha\|\mathbf{h}_{\Lambda^c}\|_2 + (1 - \gamma)\|\mathbf{h}_{\Lambda^c}\|_2^2 \leq \gamma\|\mathbf{h}_\Lambda\|_1 + \gamma\alpha\|\mathbf{h}_\Lambda\|_2 + (\gamma - 1)(\|\mathbf{h}_\Lambda\|_2^2 - 2\|\bar{\mathbf{x}}\|_2\|\mathbf{h}_\Lambda\|_2)$ . Since  $0 < \gamma < 1$ , we further obtain

$$(2.16) \quad \|\mathbf{h}_{\Lambda^c}\|_1 - \alpha\|\mathbf{h}_{\Lambda^c}\|_2 + \frac{1 - \gamma}{\gamma}(\|\mathbf{h}_{\Lambda^c}\|_2^2 + \|\mathbf{h}_\Lambda\|_2^2 - 2\|\bar{\mathbf{x}}\|_2\|\mathbf{h}_\Lambda\|_2) \leq \|\mathbf{h}_\Lambda\|_1 + \alpha\|\mathbf{h}_\Lambda\|_2.$$

We sort the components of  $\Lambda^c$  in descending order by magnitude and divide them into disjoint subsets  $\Lambda_i^c$  with cardinality  $3s$  (the last one possibly smaller), i.e.,  $\Lambda^c = \bigcup_{i=1}^{\ell} \Lambda_i^c$  and  $\Lambda_i^c \cap \Lambda_j^c = \emptyset$  for  $i \neq j$ . Let  $\Lambda_0^c = \Lambda \cup \Lambda_1^c$ . Using the RIP property of  $\mathbf{A}$  and  $\mathbf{A}\mathbf{h} = 0$ , we have  $0 = \|\mathbf{A}\mathbf{h}\|_2 \geq \|\mathbf{A}_{\Lambda_0^c}\mathbf{h}_{\Lambda_0^c}\|_2 - \left\| \sum_{i=2}^{\ell} \mathbf{A}_{\Lambda_i^c}\mathbf{h}_{\Lambda_i^c} \right\|_2 \geq \|\mathbf{A}_{\Lambda_0^c}\mathbf{h}_{\Lambda_0^c}\|_2 - \sum_{i=2}^{\ell} \|\mathbf{A}_{\Lambda_i^c}\mathbf{h}_{\Lambda_i^c}\|_2$ . Set  $A := \sqrt{1 - \delta_{4s}}$  and  $B := \sqrt{1 + \delta_{3s}}$ . It follows from the RIP condition that  $0 = \|\mathbf{A}\mathbf{h}\|_2 \geq A\|\mathbf{h}_{\Lambda_0^c}\|_2 - B\sum_{i=2}^{\ell} \|\mathbf{h}_{\Lambda_i^c}\|_2$ . By the statement (b) in Lemma 2.5, for any  $i \geq 2$  and  $t \in \Lambda_i^c$ , one has

$$\begin{aligned} |h_t| &+ \frac{(1 - \gamma)\|\mathbf{h}_{\Lambda_i^c}\|_2^2}{\gamma(3\alpha s - \alpha\sqrt{3s} + (1 - \alpha)3^p s^p H_{3s,p})} \\ &\leq \min_{r \in \Lambda_{i-1}^c} |h_r| + \frac{(1 - \gamma)\|\mathbf{h}_{\Lambda_{i-1}^c}\|_2^2}{\gamma(3\alpha s - \alpha\sqrt{3s} + (1 - \alpha)3^p s^p H_{3s,p})} \\ &\leq \frac{\gamma \left( \|\mathbf{h}_{\Lambda_{i-1}^c}\|_2 - \alpha\|\mathbf{h}_{\Lambda_{i-1}^c}\|_2 \right) + (1 - \gamma)\|\mathbf{h}_{\Lambda_{i-1}^c}\|_2^2}{\gamma(3\alpha s - \alpha\sqrt{3s} + (1 - \alpha)3^p s^p H_{3s,p})}. \end{aligned}$$

Thus, for any  $i \geq 2$ ,  $\|\mathbf{h}_{\Lambda_i^c}\|_2^2$  admits the upper bound

$$\|\mathbf{h}_{\Lambda_i^c}\|_2^2 \leq 3s \left[ \frac{\gamma(\|\mathbf{h}_{\Lambda_{i-1}^c}\|_1 - \alpha\|\mathbf{h}_{\Lambda_{i-1}^c}\|_2) + (1 - \gamma)\|\mathbf{h}_{\Lambda_{i-1}^c}\|_2^2}{\gamma(3\alpha s - \alpha\sqrt{3s} + (1 - \alpha)3^p s^p H_{3s,p})} \right]^2.$$

Summing over  $i \geq 2$  and simplifying yields

$$(2.17) \quad \begin{aligned} \sum_{i=2}^{\ell} \|\mathbf{h}_{\Lambda_i^c}\|_2 &\leq \sqrt{3s} \sum_{i=1}^{\ell-1} \frac{\gamma (\|\mathbf{h}_{\Lambda_i^c}\|_1 - \alpha \|\mathbf{h}_{\Lambda_i^c}\|_2) + (1-\gamma) \|\mathbf{h}_{\Lambda_i^c}\|_2^2}{\gamma (3\alpha s - \alpha \sqrt{3s} + (1-\alpha) 3^p s^p H_{3s,p})} \\ &\leq \sqrt{3s} \cdot \frac{\gamma \sum_{i=1}^{\ell} \|\mathbf{h}_{\Lambda_i^c}\|_1 - \gamma \alpha \sum_{i=1}^{\ell} \|\mathbf{h}_{\Lambda_i^c}\|_2 + (1-\gamma) \sum_{i=1}^{\ell} \|\mathbf{h}_{\Lambda_i^c}\|_2^2}{\gamma (3\alpha s - \alpha \sqrt{3s} + (1-\alpha) 3^p s^p H_{3s,p})}. \end{aligned}$$

By  $\sum_{i=1}^{\ell} \|\mathbf{h}_{\Lambda_i^c}\|_1 = \|\mathbf{h}_{\Lambda^c}\|_1$ ,  $(1-\gamma) \sum_{i=1}^{\ell} \|\mathbf{h}_{\Lambda_i^c}\|_2^2 = (1-\gamma) \|\mathbf{h}_{\Lambda^c}\|_2^2$ , and the inequality  $\gamma \alpha \sum_{i=1}^{\ell} \|\mathbf{h}_{\Lambda_i^c}\|_2 \geq \gamma \alpha \sqrt{\sum_{i=1}^{\ell} \|\mathbf{h}_{\Lambda_i^c}\|_2^2} = \gamma \alpha \|\mathbf{h}_{\Lambda^c}\|_2$ , and substitute (2.16) into (2.17) to obtain

$$\begin{aligned} \sum_{i=2}^{\ell} \|\mathbf{h}_{\Lambda_i^c}\|_2 &\stackrel{a}{\leq} \sqrt{3s} \cdot \frac{(\gamma \sqrt{s} + \gamma \alpha) \|\mathbf{h}_{\Lambda}\|_2 + (\gamma - 1) (\|\mathbf{h}_{\Lambda}\|_2^2 - 2 \|\mathbf{h}_{\Lambda}\|_2 \|\bar{\mathbf{x}}\|_2)}{\gamma (3\alpha s - \alpha \sqrt{3s} + (1-\alpha) 3^p s^p H_{3s,p})} \\ &\stackrel{b}{\leq} \frac{(\gamma \sqrt{s} + \gamma \alpha + 2(1-\gamma)M) \|\mathbf{h}_{\Lambda}\|_2}{\gamma (\alpha \sqrt{3s} - \alpha + (1-\alpha) 3^p s^p H_{3s,p} / \sqrt{3s})}, \end{aligned}$$

where inequality  $\stackrel{a}{\leq}$  holds due to condition  $\gamma \|\mathbf{h}_{\Lambda}\|_1 \leq \gamma \sqrt{s} \|\mathbf{h}_{\Lambda}\|_2$  and inequality  $\stackrel{b}{\leq}$  follows from the boundedness of the signal  $\bar{\mathbf{x}}$ , i.e.,  $\|\bar{\mathbf{x}}\|_2 \leq M$ . Let

$$\sqrt{a(s, \gamma, \alpha, p)} = \frac{\gamma(\alpha \sqrt{3s} - \alpha + (1-\alpha)(3s)^p H_{3s,p} / \sqrt{3s})}{\gamma \sqrt{s} + \gamma \alpha + 2(1-\gamma)M}.$$

Then  $\sum_{i=2}^{\ell} \|\mathbf{h}_{\Lambda_i^c}\|_2 \leq \frac{\|\mathbf{h}_{\Lambda}\|_2}{\sqrt{a(s, \gamma, \alpha, p)}}$ . It follows that  $0 \geq A \|\mathbf{h}_{\Lambda_0^c}\|_2 - B \sum_{i=2}^{\ell} \|\mathbf{h}_{\Lambda_i^c}\|_2 \geq A \|\mathbf{h}_{\Lambda_0^c}\|_2 - \frac{B}{\sqrt{a(s, \lambda, \alpha, p)}} \|\mathbf{h}_{\Lambda}\|_2 \stackrel{a}{\geq} \left( A - \frac{B}{\sqrt{a(s, \lambda, \alpha, p)}} \right) \|\mathbf{h}_{\Lambda_0^c}\|_2$ , where the inequality  $\stackrel{a}{\geq}$  holds because  $\|\mathbf{h}_{\Lambda_0^c}\|_2^2 = \|\mathbf{h}_{\Lambda} + \mathbf{h}_{\Lambda_1^c}\|_2^2 \geq \|\mathbf{h}_{\Lambda}\|_2^2$ . Since  $a(s, \gamma, \alpha, p) > 1$  and  $\delta_{3s} + a(s, \gamma, \alpha, p) \delta_{4s} < a(s, \gamma, \alpha, p) - 1$ , it follows that  $\sqrt{1 - \delta_{4s}} - \frac{\sqrt{1 + \delta_{3s}}}{\sqrt{a(s, \lambda, \alpha, p)}} > 0$ , which implies  $\mathbf{h}_{\Lambda_0^c} = \mathbf{0}$  and so  $\mathbf{h} = \mathbf{0}$ . This proves the uniqueness of  $\bar{\mathbf{x}}$ .  $\square$

Theorem 2.6 establishes a RIP-based sufficient condition ensuring the uniqueness of the solution recovered by the measure  $\gamma (\|\mathbf{x}\|_1 - \alpha \|\mathbf{x}\|_2) + (1-\gamma) \|\mathbf{x}\|_2^2$ . This result parallels the classical RIP condition for exact recovery in BP [4], yet it is specifically tailored to the composite nonconvex objective above. Unlike the  $\ell_1$  formulation in BP, this condition explicitly characterizes the interplay between the sparsity-inducing term  $\|\mathbf{x}\|_1 - \alpha \|\mathbf{x}\|_2$  and the quadratic regularization  $\|\mathbf{x}\|_2^2$ .

At the end of this subsection, we extend the stable recovery property of [40] to demonstrate the stable recovery property of CDCEN in the presence of measurement noise.

**THEOREM 2.7.** *Let  $\alpha \in (0, 1)$  and  $\gamma \in (0, 1)$ , and suppose that all the conditions in Theorem 2.6 are satisfied with  $\mathbf{A}\bar{\mathbf{x}} + \mathbf{e} = \mathbf{b}$ , where  $\mathbf{e} \in \mathbb{R}^m$  denotes an arbitrary noise with  $\|\mathbf{e}\|_2 \leq \tau$ . Let  $\mathbf{x}^{\text{opt}}$  be an optimal solution of the noise-aware problem*

$$\min_{\mathbf{x} \in \mathbb{R}^n} \gamma (\|\mathbf{x}\|_1 - \alpha \|\mathbf{x}\|_2) + (1-\gamma) \|\mathbf{x}\|_2^2 \quad \text{subject to} \quad \|\mathbf{A}\mathbf{x} - \mathbf{b}\|_2 \leq \tau.$$

*Then the reconstruction error admits the stability bound  $\|\mathbf{x}^{\text{opt}} - \bar{\mathbf{x}}\|_2 \leq C_s \tau$ , where the constant  $C_s$  is given by  $C_s := \frac{2\sqrt{1+a(s,\gamma,\alpha,p)}}{\sqrt{a(s,\gamma,\alpha,p)(1-\delta_{4s})}-\sqrt{1+\delta_{3s}}} > 0$ .*

*Proof.* The proof is similar to the one of [40, Theorem 2.2] and so we omit it here.  $\square$

**2.2. Sparsity and Extremality under NSP.** This subsection primarily investigates the relationship between sparsity and extremality of CDCEN and DCEN under the null space property (NSP) condition.

**DEFINITION 2.8.** For any subset  $\Lambda \subset \{1, 2, \dots, n\}$  with  $|\Lambda| = s$ , a matrix  $\mathbf{A} \in \mathbb{R}^{m \times n}$  is said to satisfy the DCEN stable null space property (DCEN-NSP) of order  $s$  if  $\|\mathbf{h}_\Lambda\|_1 \leq \kappa \|\mathbf{h}_{\Lambda^c}\|_1$  for all  $\mathbf{h} \in \ker(\mathbf{A})$ , where  $\kappa \in (0, 1)$  is a constant.

**THEOREM 2.9.** Let  $\mathbf{x}^* \in \mathbb{R}^n$  be a feasible point of the problem (1.1) with  $r := \|\mathbf{x}^*\|_2$ . Denote the support set of  $\mathbf{x}^*$  by  $\Lambda_* := \text{supp}(\mathbf{x}^*) = \{i \mid x_i^* \neq 0\}$ . For any nonzero vector  $\mathbf{h} \in \ker(\mathbf{A}) \setminus \{\mathbf{0}\}$  with  $\mathbf{h} = \mathbf{h}_{\Lambda_*} + \mathbf{h}_{\Lambda_*^c}$ , where  $\Lambda_*^c$  is the complement of  $\Lambda_*$ . Let  $s_1 := \|\mathbf{h}_{\Lambda_*}\|_1$ ,  $s_2 := \|\mathbf{h}_{\Lambda_*^c}\|_1$  and  $\kappa(r) := \gamma(1-\alpha)/[\gamma(1+\alpha)+2(1-\gamma)r] \in (0, 1)$ . If there exists a constant  $\kappa \in (0, \kappa(r))$  such that the DCEN-NSP condition  $s_1 < \kappa s_2$  holds for all  $\mathbf{h} \in \ker(\mathbf{A}) \setminus \{\mathbf{0}\}$ , then  $\mathbf{x}^*$  is the unique minimizer of the problem (1.1).

*Proof.* To show that  $\mathbf{x}^*$  is the unique minimizer of (1.1), it suffices to prove that  $r_\gamma(\mathbf{x}^* + \tau\mathbf{h}) > r_\gamma(\mathbf{x}^*)$  holds for any  $\mathbf{h} \in \ker(\mathbf{A})$  with  $\mathbf{h} \neq \mathbf{0}$  and  $\tau > 0$ . For any  $\mathbf{h} \in \ker(\mathbf{A}) \setminus \{\mathbf{0}\}$  and any  $\tau > 0$ , consider  $\mathbf{x} = \mathbf{x}^* + \tau\mathbf{h}$ . Since  $\mathbf{A}\mathbf{x}^* = \mathbf{b}$  and  $\mathbf{A}\mathbf{h} = \mathbf{0}$ , we have  $\mathbf{A}(\mathbf{x}^* + \tau\mathbf{h}) = \mathbf{A}\mathbf{x}^* + \tau\mathbf{A}\mathbf{h} = \mathbf{b}$ , which means that  $\mathbf{x}$  is still feasible. Let the increment of the objective function as  $\Delta(\tau) := r_\gamma(\mathbf{x}^* + \tau\mathbf{h}) - r_\gamma(\mathbf{x}^*)$ . Then

$$(2.18) \quad \begin{aligned} \Delta(\tau) &= \gamma(\|\mathbf{x}^* + \tau\mathbf{h}\|_1 - \|\mathbf{x}^*\|_1) - \gamma\alpha(\|\mathbf{x}^* + \tau\mathbf{h}\|_2 - \|\mathbf{x}^*\|_2) \\ &\quad + (1 - \gamma)(\|\mathbf{x}^* + \tau\mathbf{h}\|_2^2 - \|\mathbf{x}^*\|_2^2). \end{aligned}$$

Since  $\mathbf{x}_{\Lambda_*^c}^* = \mathbf{0}$ , it is easy to have  $\|\mathbf{x}^* + \tau\mathbf{h}\|_1 = \|\mathbf{x}_{\Lambda_*}^* + \tau\mathbf{h}_{\Lambda_*}\|_1 + \tau\|\mathbf{h}_{\Lambda_*^c}\|_1$ . By the fact  $\|\mathbf{x}_{\Lambda_*}^* + \tau\mathbf{h}_{\Lambda_*}\|_1 \geq \|\mathbf{x}_{\Lambda_*}^*\|_1 - \tau\|\mathbf{h}_{\Lambda_*}\|_1 = \|\mathbf{x}^*\|_1 - \tau\|\mathbf{h}_{\Lambda_*}\|_1$ , it follows that  $\|\mathbf{x}^* + \tau\mathbf{h}\|_1 - \|\mathbf{x}^*\|_1 \geq \tau\|\mathbf{h}_{\Lambda_*^c}\|_1 - \tau\|\mathbf{h}_{\Lambda_*}\|_1 = \tau(s_2 - s_1)$  and so

$$(2.19) \quad \gamma(\|\mathbf{x}^* + \tau\mathbf{h}\|_1 - \|\mathbf{x}^*\|_1) \geq \gamma\tau(s_2 - s_1).$$

For the term  $-\gamma\alpha(\|\mathbf{x}^* + \tau\mathbf{h}\|_2 - \|\mathbf{x}^*\|_2)$ , by the triangle inequality, we have  $\|\mathbf{x}^* + \tau\mathbf{h}\|_2 - \|\mathbf{x}^*\|_2 \leq \tau\|\mathbf{h}\|_2 = \tau\sigma$  and so

$$(2.20) \quad -\gamma\alpha(\|\mathbf{x}^* + \tau\mathbf{h}\|_2 - \|\mathbf{x}^*\|_2) \geq -\gamma\alpha\tau\sigma,$$

where  $\sigma := \|\mathbf{h}\|_2$ . For the quadratic term  $(1 - \gamma)\|\mathbf{x}\|_2^2$ , its expansion gives  $\|\mathbf{x}^* + \tau\mathbf{h}\|_2^2 - \|\mathbf{x}^*\|_2^2 = 2\tau\mathbf{x}^{*\top}\mathbf{h} + \tau^2\|\mathbf{h}\|_2^2$ . It follows that  $(1 - \gamma)(\|\mathbf{x}^* + \tau\mathbf{h}\|_2^2 - \|\mathbf{x}^*\|_2^2) = 2(1 - \gamma)\tau\mathbf{x}^{*\top}\mathbf{h} + (1 - \gamma)\tau^2\sigma^2$ . Noting that  $\mathbf{x}^{*\top}\mathbf{h} = \mathbf{x}_{\Lambda_*}^{*\top}\mathbf{h}_{\Lambda_*}$ , by the Cauchy-Schwarz inequality we have  $|\mathbf{x}_{\Lambda_*}^{*\top}\mathbf{h}_{\Lambda_*}| \leq \|\mathbf{x}_{\Lambda_*}^*\|_2 \|\mathbf{h}_{\Lambda_*}\|_2 \leq r\|\mathbf{h}_{\Lambda_*}\|_1 = rs_1$ , and using  $\|\mathbf{h}_{\Lambda_*}\|_2 \leq \|\mathbf{h}_{\Lambda_*}\|_1$ , we further obtain

$$(2.21) \quad (1 - \gamma)(\|\mathbf{x}^* + \tau\mathbf{h}\|_2^2 - \|\mathbf{x}^*\|_2^2) \geq -2(1 - \gamma)\tau rs_1 + (1 - \gamma)\tau^2\sigma^2.$$

Combining the inequalities (2.19), (2.20), and (2.21), we have  $\Delta(\tau) \geq \gamma\tau(s_2 - s_1) - \gamma\alpha\tau\sigma - 2(1 - \gamma)\tau rs_1 + (1 - \gamma)\tau^2\sigma^2$ . This leads to a quadratic lower bound  $\Delta(\tau) \geq \tau(\gamma(s_2 - s_1) - \gamma\alpha\sigma - 2(1 - \gamma)rs_1) + (1 - \gamma)\tau^2\sigma^2$ . Since  $\sigma = \|\mathbf{h}\|_2 \leq \|\mathbf{h}\|_1 = \|\mathbf{h}_{\Lambda_*}\|_1 + \|\mathbf{h}_{\Lambda_*^c}\|_1 = s_1 + s_2$ , we have

$$(2.22) \quad \gamma(s_2 - s_1) - \gamma\alpha\sigma - 2(1 - \gamma)rs_1 \geq \gamma(s_2 - s_1) - \gamma\alpha(s_1 + s_2) - 2(1 - \gamma)rs_1.$$

Substituting  $s_1 < \kappa s_2$  into the inequality (2.22) gives  $\gamma(1 - \alpha)s_2 - (\gamma(1 + \alpha) + 2(1 - \gamma)r)s_1 \geq \gamma(1 - \alpha)s_2 - (\gamma(1 + \alpha) + 2(1 - \gamma)r)\kappa(r)s_2 = 0$ . Thus, the right-hand side of (2.18) is strictly positive, implying  $\Delta(\tau) > 0$  for all  $\tau > 0$  and  $\mathbf{h} \in \ker(\mathbf{A}) \setminus \{\mathbf{0}\}$ .

For any other feasible point  $\mathbf{x}' \neq \mathbf{x}^*$ , let  $\mathbf{h} = \mathbf{x}' - \mathbf{x}^* \in \ker(\mathbf{A})$  and choose  $\tau = 1$  in (2.18). Then  $r_\gamma(\mathbf{x}') - r_\gamma(\mathbf{x}^*) = \Delta(1) > 0$  and so  $\mathbf{x}^*$  is the unique global minimizer of (1.1).  $\square$

**COROLLARY 2.10.** *Let  $\mathbf{x}^*$  be a strict local minimizer of problem (1.1) with  $r = \|\mathbf{x}^*\|_2$ , and denote its support by  $\Lambda_* = \text{supp}(\mathbf{x}^*)$ . If the matrix  $\mathbf{A}$  satisfies*

$$(2.23) \quad \|\mathbf{h}_{\Lambda_*}\|_1 < \kappa \|\mathbf{h}_{\Lambda_*^c}\|_1, \quad \kappa \in (0, \kappa(r)),$$

for all nonzero  $\mathbf{h} \in \ker(\mathbf{A})$ , then the submatrix  $\mathbf{A}_{\Lambda_*}$  formed by the columns indexed by  $\Lambda_*$  is of full column rank, i.e.,  $\text{rank}(\mathbf{A}_{\Lambda_*}) = |\Lambda_*|$ .

*Proof.* We prove the corollary by contradiction. If the submatrix  $\mathbf{A}_{\Lambda_*}$  is not of full column rank, there exists a nonzero vector  $\mathbf{u} \in \mathbb{R}^{|\Lambda_*|}$  such that  $\mathbf{A}_{\Lambda_*}\mathbf{u} = 0$ . Extend  $\mathbf{u}$  to a vector  $\mathbf{h} \in \mathbb{R}^n$  by setting  $\mathbf{h}_{\Lambda_*} = \mathbf{u}$  and  $\mathbf{h}_{\Lambda_*^c} = \mathbf{0}$ . For this  $\mathbf{h}$ , we have  $\|\mathbf{h}_{\Lambda_*}\|_1 > 0$  and  $\|\mathbf{h}_{\Lambda_*^c}\|_1 = 0$ , which contradicts. Hence,  $\mathbf{A}_{\Lambda_*}$  must have linearly independent columns.  $\square$

**Remark 2.11.** This corollary indicates that the condition (2.23) not only provides a sufficient criterion for strict local optimality but also ensures algebraic consistency between the measurement matrix  $\mathbf{A}$  and the sparsity pattern of the solution: the columns corresponding to the support must be linearly independent; otherwise, a non-zero vector existing only on the support would lie in  $\ker(\mathbf{A})$ , violating the inequality condition.

**COROLLARY 2.12.** *Let  $\mathbf{x}^*$  be a strict local minimizer of problem (1.2). If the matrix  $\mathbf{A}$  satisfies (2.23) for all nonzero  $\mathbf{h} \in \ker(\mathbf{A})$ , then the submatrix  $\mathbf{A}_{\Lambda_*}$  is of full column rank.*

*Proof.* We claim that  $\mathbf{x}^*$  is also a local minimizer of the following constrained problem

$$\min_{\mathbf{x} \in \mathbb{R}^n} \gamma(\|\mathbf{x}\|_1 - \alpha\|\mathbf{x}\|_2) + (1 - \gamma)\|\mathbf{x}\|_2^2 \quad \text{subject to} \quad \mathbf{A}\mathbf{x} = \mathbf{A}\mathbf{x}^* = \mathbf{b}.$$

Suppose not. Then  $\forall \tilde{r} > 0$ , there exists  $\tilde{\mathbf{x}} \in \mathcal{B}_{\tilde{r}}(\mathbf{x}^*)$  such that  $\mathbf{A}\tilde{\mathbf{x}} = \mathbf{A}\mathbf{x}^*$  and  $\gamma(\|\tilde{\mathbf{x}}\|_1 - \alpha\|\tilde{\mathbf{x}}\|_2) + (1 - \gamma)\|\tilde{\mathbf{x}}\|_2^2 < \gamma(\|\mathbf{x}^*\|_1 - \alpha\|\mathbf{x}^*\|_2) + (1 - \gamma)\|\mathbf{x}^*\|_2^2$ . This implies  $\frac{1}{2}\|\mathbf{A}\tilde{\mathbf{x}} - \mathbf{b}\|_2^2 + \lambda(\gamma(\|\tilde{\mathbf{x}}\|_1 - \alpha\|\tilde{\mathbf{x}}\|_2) + (1 - \gamma)\|\tilde{\mathbf{x}}\|_2^2) < \frac{1}{2}\|\mathbf{A}\mathbf{x}^* - \mathbf{b}\|_2^2 + \lambda(\gamma(\|\mathbf{x}^*\|_1 - \alpha\|\mathbf{x}^*\|_2) + (1 - \gamma)\|\mathbf{x}^*\|_2^2)$ . Thus for any  $\tilde{r} > 0$ , we actually find a  $\tilde{\mathbf{x}} \in \mathcal{B}_{\tilde{r}}(\mathbf{x}^*)$  yielding a smaller objective of (1.2) than  $\mathbf{x}^*$ , which leads to a contradiction because  $\mathbf{x}^*$  is assumed to be a local minimizer. Thus the claim is validated. Using the claim above and Corollary 2.10, we have that the columns of  $\mathbf{A}_{\Lambda_*}$  are linearly independent.  $\square$

**3. Proximal Operator.** In this section, we derive a closed-form expression for the proximal operator of the DCEN regularization defined as

$$(3.1) \quad \text{prox}_{\lambda r_\gamma}(\mathbf{y}) = \arg \min_{\mathbf{x} \in \mathbb{R}^n} \gamma(\|\mathbf{x}\|_1 - \alpha\|\mathbf{x}\|_2) + (1 - \gamma)\|\mathbf{x}\|_2^2 + \frac{1}{2\lambda}\|\mathbf{x} - \mathbf{y}\|_2^2,$$

with  $\lambda > 0$ . To this end, we first show the following existence of solutions of (3.1).

**THEOREM 3.1** (Solution's Existence). *Let  $\lambda > 0$ ,  $\gamma \in (0, 1)$ ,  $\alpha \in (0, 1)$ , and  $\mathbf{y} \in \mathbb{R}^n$  be given. Then the solution set of the minimization problem (3.1) is nonempty, i.e.,  $\text{prox}_{\lambda r_\gamma}(\mathbf{y}) \neq \emptyset$ .*

*Proof.* Clearly, the objective function in (3.1) is proper and closed. It follows from the inequality  $\|\mathbf{x}\|_1 \geq \|\mathbf{x}\|_2$  that  $f_{\gamma,\alpha}(\mathbf{x}) = \gamma\|\mathbf{x}\|_1 - \gamma\alpha\|\mathbf{x}\|_2 + (1-\gamma)\|\mathbf{x}\|_2^2 + \frac{1}{2\lambda}\|\mathbf{x} - \mathbf{y}\|_2^2 \geq (1-\gamma + \frac{1}{2\lambda})\|\mathbf{x}\|_2^2 + [\gamma(1-\alpha) - \frac{1}{\lambda}\|\mathbf{y}\|_2]\|\mathbf{x}\|_2 + \frac{1}{2\lambda}\|\mathbf{y}\|_2^2$ . The right-hand side is a quadratic function of  $\|\mathbf{x}\|_2$  with a positive leading coefficient  $1-\gamma + \frac{1}{2\lambda} > 0$ . Hence,  $f_{\gamma,\alpha}(\mathbf{x}) \rightarrow +\infty$  as  $\|\mathbf{x}\|_2 \rightarrow \infty$ , which implies that  $f_{\gamma,\alpha}$  is coercive. Since  $f_{\gamma,\alpha}$  is also lower semicontinuous, its sublevel sets are compact and so  $\text{prox}_{\lambda r_\gamma}(\mathbf{y}) \neq \emptyset$ .  $\square$

LEMMA 3.2. *Let  $\mathbf{y} \in \mathbb{R}^n$ ,  $\lambda > 0$ ,  $\gamma \in (0, 1)$ , and  $\alpha \geq 0$ . Denote by  $\mathbf{x}^*$  an optimal solution to problem (1.2). Then  $\mathbf{x}^*$  admits the following characterization.*

- (a) *If  $\|\mathbf{y}\|_\infty > \gamma\lambda$ , then  $\mathbf{x}^* = \frac{\|\mathcal{S}_{\gamma\lambda}(\mathbf{y})\|_2 + \alpha\gamma\lambda}{(1+2\lambda(1-\gamma))\|\mathcal{S}_{\gamma\lambda}(\mathbf{y})\|_2} \mathcal{S}_{\gamma\lambda}(\mathbf{y})$ , where  $\mathcal{S}_{\gamma\lambda}(\mathbf{y}) = \text{sign}(\mathbf{y}) \odot \max(|\mathbf{y}| - \gamma\lambda, \mathbf{0})$ .*
- (b) *If  $\|\mathbf{y}\|_\infty = \gamma\lambda$ , then the optimal solution  $\mathbf{x}^*$  satisfies  $\mathbf{x}^* \in \left\{ \mathbf{x} \in \mathbb{R}^n : x_i = 0 \text{ for } |y_i| < \gamma\lambda, \|\mathbf{x}\|_2 = \alpha\gamma\lambda, x_i y_i \geq 0, \forall i \right\}$ , and  $\mathbf{x}^*$  is non-unique if multiple  $|y_i| = \gamma\lambda$ .*
- (c) *If  $(1-\alpha)\gamma\lambda < \|\mathbf{y}\|_\infty < \gamma\lambda$ , then  $\mathbf{x}^*$  is 1-sparse, supported on an index  $i$  with  $|y_i| = \|\mathbf{y}\|_\infty$ , and  $\mathbf{x}^* \in \left\{ \mathbf{x} \in \mathbb{R}^n : \|\mathbf{x}\|_2 = \|\mathbf{y}\|_\infty + (\alpha-1)\gamma\lambda, x_i y_i \geq 0 \right\}$ .*
- (d) *If  $\|\mathbf{y}\|_\infty \leq (1-\alpha)\gamma\lambda$ , then  $\mathbf{x}^* = \mathbf{0}$ .*

*Proof.* By combining the quadratic terms in the proximal mapping (3.1), the resulting operator can be expressed in the same form as the  $\ell_1 - \alpha\ell_2$  proximal mapping  $\text{prox}_{\lambda r_\gamma}(\tilde{\mathbf{y}}) = \arg \min_{\mathbf{x} \in \mathbb{R}^n} \|\mathbf{x}\|_1 - \alpha\|\mathbf{x}\|_2 + \frac{1}{2\lambda}\|\mathbf{x} - \tilde{\mathbf{y}}\|_2^2$ , where  $\lambda = \frac{\lambda\gamma}{1+2\beta(1-\gamma)}$  and  $\tilde{\mathbf{y}} = \frac{1}{1+2\beta(1-\gamma)}\mathbf{y}$ . This reformulation allows one to directly apply the closed-form expressions derived for the  $\ell_1 - \alpha\ell_2$  case. The remaining proof follows that of [24] and is therefore omitted.  $\square$

*Remark 3.3.* When  $\alpha = 0$  and  $\gamma = 1$ , the analytical solution of the proximal operator  $\text{prox}_{\lambda r_\gamma}$  degenerates to the soft-thresholding function  $\mathcal{S}_\lambda(\mathbf{y}, \lambda)$  associated with the  $\ell_1$  norm. When  $\alpha = 0$  and  $\gamma \in (0, 1)$ , the analytical solution of  $\text{prox}_{\lambda r_\gamma}$  specializes to the soft-thresholding function of Elastic Net. When  $\alpha > 0$  and  $\gamma = 1$ , the closed-form of  $\text{prox}_{\lambda r_\gamma}$  coincides with that of the  $\ell_1 - \alpha\ell_2$  proximal operator. This lemma can thus be viewed as a direct generalization of Lemma 1 in [24] and Lemma 1 in [22].

LEMMA 3.4. *Given  $\mathbf{y} \in \mathbb{R}^n$ ,  $\lambda > 0$ ,  $\gamma \in (0, 1)$ , and  $\alpha \geq 0$ . If  $\mathbf{x}^* \in \text{prox}_{\lambda r_\gamma}(\mathbf{y})$  be the minimizer. Then, for any  $\mathbf{x} \in \mathbb{R}^n$ , the quadratic upper bound  $f_{\gamma,\alpha}(\mathbf{x}^*) - f_{\gamma,\alpha}(\mathbf{x}) \leq \min \frac{1}{2} \left( \frac{\gamma\alpha}{\|\mathbf{x}^*\|_2} - \frac{1}{\lambda} - (1-\gamma), 0 \right) \|\mathbf{x}^* - \mathbf{x}\|_2^2$  holds, where  $\frac{\gamma\alpha}{0}$  is defined as 0 if  $\alpha = 0$ , and  $+\infty$  if  $\alpha > 0$ .*

*Proof.* We consider two cases based on the support of  $\mathbf{x}^*$ .

**Case 1:  $\mathbf{x}^* \neq \mathbf{0}$ .** Since  $\mathbf{x}^*$  is a minimizer of  $f_{\gamma,\alpha}$ , according to the first-order optimality condition, we have  $\mathbf{0} \in \gamma\partial\|\mathbf{x}^*\|_1 - \gamma\alpha\frac{\mathbf{x}^*}{\|\mathbf{x}^*\|_2} + 2(1-\gamma)\mathbf{x}^* + \frac{1}{\lambda}(\mathbf{x}^* - \mathbf{y})$ . Thus, there exists  $\mathbf{p} \in \partial\|\mathbf{x}^*\|_1$  such that

$$(3.2) \quad \mathbf{p} = \frac{1}{\lambda\gamma}\mathbf{y} - \left( \frac{1}{\lambda\gamma} + \frac{2(1-\gamma)}{\gamma} - \frac{\gamma\alpha}{\|\mathbf{x}^*\|_2} \right) \mathbf{x}^*.$$

By the subgradient inequality for  $\|\cdot\|_1$ , one has  $\|\mathbf{x}\|_1 \geq \|\mathbf{x}^*\|_1 + \langle \mathbf{p}, \mathbf{x} - \mathbf{x}^* \rangle$ , which implies  $\|\mathbf{x}^*\|_1 - \|\mathbf{x}\|_1 \leq \langle \mathbf{p}, \mathbf{x}^* - \mathbf{x} \rangle$  and so  $f_{\gamma,\alpha}(\mathbf{x}^*) - f_{\gamma,\alpha}(\mathbf{x}) \leq \gamma\langle \mathbf{p}, \mathbf{x}^* - \mathbf{x} \rangle - \gamma\alpha(\|\mathbf{x}^*\|_2 - \|\mathbf{x}\|_2) + (1-\gamma)(\|\mathbf{x}^*\|_2^2 - \|\mathbf{x}\|_2^2) + \frac{1}{2\lambda}(\|\mathbf{x}^* - \mathbf{y}\|_2^2 - \|\mathbf{x} - \mathbf{y}\|_2^2)$ . Substitute the expression for  $\mathbf{p}$  from (3.2) into the first term, one has  $\gamma\langle \mathbf{p}, \mathbf{x}^* - \mathbf{x} \rangle = \gamma\langle \frac{\mathbf{y} - \mathbf{x}^*}{\lambda\gamma} - \frac{1}{\lambda\gamma}\mathbf{y} + \left( \frac{1}{\lambda\gamma} + \frac{2(1-\gamma)}{\gamma} - \frac{\gamma\alpha}{\|\mathbf{x}^*\|_2} \right) \mathbf{x}^*, \mathbf{x}^* - \mathbf{x} \rangle = \gamma\langle \frac{\mathbf{y} - \mathbf{x}^*}{\lambda\gamma} - \frac{1}{\lambda\gamma}\mathbf{y}, \mathbf{x}^* - \mathbf{x} \rangle + \gamma\left( \frac{1}{\lambda\gamma} + \frac{2(1-\gamma)}{\gamma} - \frac{\gamma\alpha}{\|\mathbf{x}^*\|_2} \right) \|\mathbf{x}^* - \mathbf{x}\|_1$ .

$\frac{2(1-\gamma)\mathbf{x}^*}{\gamma} + \frac{\alpha\mathbf{x}^*}{\|\mathbf{x}^*\|_2}, \mathbf{x}^* - \mathbf{x}\rangle$ . It follows from  $\frac{1}{2\lambda} (\|\mathbf{x}^* - \mathbf{y}\|_2^2 - \|\mathbf{x} - \mathbf{y}\|_2^2) = -\frac{1}{2\lambda} \|\mathbf{x}^* - \mathbf{x}\|_2^2 + \frac{1}{\lambda} \langle \mathbf{x}^* - \mathbf{y}, \mathbf{x}^* - \mathbf{x} \rangle$  that  $f_{\gamma,\alpha}(\mathbf{x}^*) - f_{\gamma,\alpha}(\mathbf{x}) = \gamma \frac{\alpha}{\|\mathbf{x}^*\|_2} (-\langle \mathbf{x}^*, \mathbf{x} \rangle + \|\mathbf{x}^*\|_2 \|\mathbf{x}\|_2) - (1 - \gamma) (\|\mathbf{x}^*\|_2^2 + \|\mathbf{x}\|_2^2) - \frac{1}{2\lambda} \|\mathbf{x}^* - \mathbf{x}\|_2^2$ . From the basic inequalities  $\|\mathbf{x}^*\|_2^2 + \|\mathbf{x}\|_2^2 \geq \frac{1}{2} \|\mathbf{x}^* - \mathbf{x}\|_2^2$  and  $\|\mathbf{x}^*\|_2 \|\mathbf{x}\|_2 \leq \frac{1}{2} \|\mathbf{x}^*\|_2^2 + \frac{1}{2} \|\mathbf{x}\|_2^2$ , we have  $\gamma \frac{\alpha}{\|\mathbf{x}^*\|_2} (-\langle \mathbf{x}^*, \mathbf{x} \rangle + \|\mathbf{x}^*\|_2 \|\mathbf{x}\|_2) - (1 - \gamma) (\|\mathbf{x}^*\|_2^2 + \|\mathbf{x}\|_2^2) - \frac{1}{2\lambda} \|\mathbf{x}^* - \mathbf{x}\|_2^2 = \frac{1}{2} \left( \frac{\gamma\alpha}{\|\mathbf{x}^*\|_2} - \frac{1}{\lambda} - (1 - \gamma) \right)$ .

**Case 2:  $\mathbf{x}^* = \mathbf{0}$ .** It follows from  $f_{\gamma,\alpha}(\mathbf{0}) \leq f_{\gamma,\alpha}(\mathbf{x})$  that  $f_{\gamma,\alpha}(\mathbf{x}^*) - f_{\gamma,\alpha}(\mathbf{x}) \leq 0$ . In the special case  $\alpha = 0$ , expanding  $f_{\gamma,\alpha}(\mathbf{0}) - f_{\gamma,\alpha}(\mathbf{x})$  yields  $f_{\gamma,\alpha}(\mathbf{0}) - f_{\gamma,\alpha}(\mathbf{x}) = \frac{1}{\lambda} \langle \mathbf{x}, \mathbf{y} \rangle - \gamma \|\mathbf{x}\|_1 - (1 - \gamma + \frac{1}{2\lambda}) \|\mathbf{x}\|_2^2$ . According to statement (d) in Lemma 3.2, we have  $\|\mathbf{y}\|_\infty \leq \gamma\lambda$ , which implies that  $\langle \mathbf{x}, \mathbf{y} \rangle \leq \gamma\lambda \|\mathbf{x}\|_1$  and  $\frac{1}{\lambda} \langle \mathbf{x}, \mathbf{y} \rangle - \gamma \|\mathbf{x}\|_1 \leq 0$ . It follows that  $f_{\gamma,\alpha}(\mathbf{0}) - f_{\gamma,\alpha}(\mathbf{x}) \leq - (1 - \gamma + \frac{1}{2\lambda}) \|\mathbf{x}\|_2^2 \leq 0$ . Combining both cases, since  $f_{\gamma,\alpha}(\mathbf{x}^*) - f_{\gamma,\alpha}(\mathbf{x}) \leq 0$  always holds, and in Case 1 it is bounded by a quadratic term, the uniform bound is  $f_{\gamma,\alpha}(\mathbf{x}^*) - f_{\gamma,\alpha}(\mathbf{x}) \leq \min \left( \frac{1}{2} \left( \frac{\gamma\alpha}{\|\mathbf{x}^*\|_2} - \frac{1}{\lambda} - (1 - \gamma) \right), 0 \right) \|\mathbf{x}^* - \mathbf{x}\|_2^2$ . When  $\gamma = 1$ , Lemma 3.4 degenerates into Lemma 2 in [24].  $\square$

**4. DC algorithm.** This section presents DC algorithm (DCA) for DCEN and shows its global convergence and linear convergence rate within the KL framework.

**4.1. DC decomposition and iteration framework.** DCA can be expressed as the difference of two proper and convex functions, i.e.,  $f(\mathbf{x}) = g(\mathbf{x}) - h(\mathbf{x})$ . At each iteration, DCA linearizes the concave part  $-h(\mathbf{x})$  using a subgradient  $\mathbf{y}^k \in \partial h(\mathbf{x}^k)$  and solves a convex subproblem  $\mathbf{x}^{k+1} \in \arg \min_{\mathbf{x} \in \mathbb{R}^n} \{g(\mathbf{x}) - \langle \mathbf{y}^k, \mathbf{x} \rangle\}$ . The standard iterative framework of DCA is given by

$$\mathbf{x}^{k+1} = \arg \min_{\mathbf{x} \in \mathbb{R}^n} g(\mathbf{x}) - (h(\mathbf{x}^k) + \langle \mathbf{y}^k, \mathbf{x} - \mathbf{x}^k \rangle), \quad \mathbf{y}^k \in \partial h(\mathbf{x}^k).$$

The objective function of the unconstrained optimization problem (1.2) takes the form

$$(4.1) \quad \mathcal{H}(\mathbf{x}) = \underbrace{\frac{1}{2} \|\mathbf{Ax} - \mathbf{b}\|_2^2 + \lambda \left( \gamma \|\mathbf{x}\|_1 + \frac{3(1-\gamma)}{2} \|\mathbf{x}\|_2^2 \right)}_{g(\mathbf{x})} - \underbrace{\lambda \left( \alpha\gamma \|\mathbf{x}\|_2 + \frac{1-\gamma}{2} \|\mathbf{x}\|_2^2 \right)}_{h(\mathbf{x})},$$

which is a DC function, amenable to optimization via DCA. Let  $\mathbf{d}_{\ell_2}(\mathbf{x}_k) = (\alpha\gamma/\|\mathbf{x}_k\|_2 + 1 - \gamma)\mathbf{x}_k$ . The update of DCA for minimizing  $\mathcal{H}(\mathbf{x})$  takes the form

$$(4.2) \quad \mathbf{x}_{k+1} = \begin{cases} \arg \min_{\mathbf{x} \in \mathbb{R}^n} g(\mathbf{x}), & \text{if } \mathbf{x}_k = 0, \\ \arg \min_{\mathbf{x} \in \mathbb{R}^n} g(\mathbf{x}) - \lambda \langle \mathbf{x}, \mathbf{d}_{\ell_2}(\mathbf{x}_k) \rangle, & \text{otherwise,} \end{cases}$$

which follows from linearizing the concave term  $-\lambda (\alpha\gamma \|\mathbf{x}\|_2 + \frac{1-\gamma}{2} \|\mathbf{x}\|_2^2)$  at  $\mathbf{x}_k$ . We adopt the effective stopping criterion  $\|\mathbf{x}_{k+1} - \mathbf{x}_k\|_2 \leq \epsilon(1 + \|\mathbf{x}_k\|_2)$ , where  $\epsilon > 0$  is a prescribed tolerance. The detailed procedure for minimizing DCEN (DCEN-DCA) is presented in Algorithm 4.1.

**4.2. ADMM solver for the subproblem in DCEN-DCA.** At each iteration of DCEN-DCA, the concave part of the DC decomposition is linearized at the current point, leading to a convex optimization subproblem

$$(4.3) \quad \mathbf{x}_{k+1} \in \arg \min_{\mathbf{x} \in \mathbb{R}^n} \frac{1}{2} \|\mathbf{Ax} - \mathbf{b}\|_2^2 + \lambda \left( \gamma \|\mathbf{x}\|_1 + \frac{3(1-\gamma)}{2} \|\mathbf{x}\|_2^2 \right) - \lambda \langle \mathbf{x}, \mathbf{d}_{\ell_2}(\mathbf{x}_k) \rangle.$$

**Algorithm 4.1** DCEN-DCA

---

**Require:** Initialize  $\mathbf{A}, \mathbf{b}, \mathbf{x}_0, \epsilon > 0, \lambda > 0, \alpha \in (0, 1)$ , and  $\gamma \in (0, 1)$ .

- 1: **for**  $k = 1$  to  $K$  **do**
- 2:   **if**  $\mathbf{x}_k = \mathbf{0}$  **then**
- 3:      $\mathbf{x}_{k+1} \leftarrow \arg \min_{\mathbf{x} \in \mathbb{R}^n} g(\mathbf{x})$
- 4:   **else**
- 5:      $\mathbf{x}_{k+1} \leftarrow \arg \min_{\mathbf{x} \in \mathbb{R}^n} \{g(\mathbf{x}) - \lambda \langle \mathbf{x}, \mathbf{d}_{\ell_2}(\mathbf{x}_k) \rangle\}$
- 6:   **end if**
- 7: **end for**

---

In the proposed DCEN-DCA iterator framework, this convex subproblem admits a solution via ADMM. Specifically, we introduce an auxiliary variable  $\mathbf{z}$  to decouple the  $\ell_1$  norm term. The subproblem (4.3) is then equivalently reformulated as the following constrained optimization problem

$$\min_{\mathbf{x}, \mathbf{z} \in \mathbb{R}^n} \frac{1}{2} \|\mathbf{Ax} - \mathbf{b}\|_2^2 + \frac{3\lambda(1-\gamma)}{2} \|\mathbf{x}\|_2^2 - \lambda \langle \mathbf{x}, \mathbf{d}_{\ell_2}(\mathbf{x}_k) \rangle + \lambda\gamma \|\mathbf{z}\|_1 \text{ s.t. } \mathbf{x} - \mathbf{z} = \mathbf{0}.$$

The augmented Lagrangian function with penalty parameter  $\rho > 0$  and dual variable  $\mathbf{y}$  is given by  $\mathcal{L}_\rho(\mathbf{x}, \mathbf{z}, \mathbf{y}) = \frac{1}{2} \|\mathbf{Ax} - \mathbf{b}\|_2^2 + \frac{3\lambda(1-\gamma)}{2} \|\mathbf{x}\|_2^2 - \lambda \langle \mathbf{x}, \mathbf{d}_{\ell_2}(\mathbf{x}_k) \rangle + \lambda\gamma \|\mathbf{z}\|_1 + \langle \mathbf{y}, \mathbf{x} - \mathbf{z} \rangle + \frac{\rho}{2} \|\mathbf{x} - \mathbf{z}\|_2^2$ . Let  $f(\mathbf{x}) = \frac{1}{2} \|\mathbf{Ax} - \mathbf{b}\|_2^2 + \frac{3\lambda(1-\gamma)}{2} \|\mathbf{x}\|_2^2$ . Then at the  $t$ -th iteration of ADMM (with the outer DCEN-DCA index  $k$  suppressed for clarity), the primal and dual variables are updated according to

$$(4.4) \quad \begin{cases} \mathbf{x}_{t+1} = \arg \min_{\mathbf{x} \in \mathbb{R}^n} f(\mathbf{x}) - \lambda \mathbf{x}^\top \mathbf{d}_{\ell_2}(\mathbf{x}_k) + \mathbf{y}_k^\top \mathbf{x} + \frac{\rho}{2} \|\mathbf{x} - \mathbf{z}_k\|_2^2, \\ \mathbf{z}_{t+1} = \arg \min_{\mathbf{z} \in \mathbb{R}^n} \frac{\rho}{2} \|\mathbf{x}_{t+1} - \mathbf{z}\|_2^2 + \lambda\gamma \|\mathbf{z}\|_1 + \langle \mathbf{y}_k, \mathbf{x}_{t+1} - \mathbf{z} \rangle, \\ \mathbf{y}_{t+1} = \mathbf{y}_t + \rho(\mathbf{x}_{t+1} - \mathbf{z}_{t+1}). \end{cases}$$

As for the  $\mathbf{x}$ -subproblem of (4.4), the closed form solution is  $\mathbf{x}_{t+1} = (\mathbf{A}^\top \mathbf{A} + (3\lambda(1-\gamma) + \rho)\mathbf{I})^{-1} (\mathbf{A}^\top \mathbf{b} + \lambda \mathbf{d}_{\ell_2}(\mathbf{x}_k) - \mathbf{y}_t + \rho \mathbf{z}_t)$ . Let  $\eta = 3\lambda(1-\gamma) + \rho$  and  $\mathbf{R}_t = \mathbf{A}^\top \mathbf{b} + \lambda \mathbf{d}_{\ell_2}(\mathbf{x}_k) - \mathbf{y}_t + \rho \mathbf{z}_t$ . By applying the Sherman–Morrison–Woodbury (SMW) identity, we have  $\mathbf{x}_{t+1} = \eta^{-1} \mathbf{R}_t - \eta^{-2} \mathbf{A}^\top (\mathbf{I} + \eta^{-1} \mathbf{A} \mathbf{A}^\top)^{-1} \mathbf{A} \mathbf{R}_t$ . For moderate  $n$  precompute a Cholesky factorization of the matrix  $\mathbf{A}^\top \mathbf{A} + (3\lambda(1-\gamma) + \rho)\mathbf{I}$  and for large-scale problems use conjugate gradient (CG) with warm start.

For the  $\mathbf{z}$ -update

$$\begin{aligned} \mathbf{z}_{t+1} &= \arg \min_{\mathbf{z} \in \mathbb{R}^n} \frac{\rho}{2} \|\mathbf{x}_{t+1} - \mathbf{z}\|_2^2 + \lambda\gamma \|\mathbf{z}\|_1 + \langle \mathbf{y}_t, \mathbf{x}_{t+1} - \mathbf{z} \rangle \\ &= \arg \min_{\mathbf{z} \in \mathbb{R}^n} \|\mathbf{z}\|_1 + \frac{\rho}{2\lambda\gamma} \|\mathbf{z} - (\mathbf{x}_{t+1} + 1/\rho \mathbf{y}_t)\|_2^2, \end{aligned}$$

which has a solution  $\mathbf{z}_{t+1} := \text{sign}(\mathbf{x}_{t+1} + \rho^{-1} \mathbf{y}_t) \odot \max\left(|\mathbf{x}_{t+1} + \rho^{-1} \mathbf{y}_t| - \frac{\lambda\gamma}{\rho}, \mathbf{0}\right)$ .

The inner ADMM iteration is terminated at step  $t$  when the primal and dual feasibility, together with the relative consistency, are simultaneously satisfied

$$(4.5) \quad \|\mathbf{r}_t\|_2 \leq \varepsilon_{\text{pri}}^t, \quad \|\mathbf{s}_t\|_2 \leq \varepsilon_{\text{dual}}^t, \text{ and } \text{relerr}_t < \varepsilon_{\text{rel}},$$

where  $\mathbf{r}_t = \mathbf{x}_t - \mathbf{z}_t$  and  $\mathbf{s}_t = \rho(\mathbf{z}_t - \mathbf{z}_{t-1})$ . The primal and dual residuals, as well as

---

**Algorithm 4.2** ADMM for minimizing DCEN-DCA subproblem (4.3).

---

**Require:**  $\mathbf{A}, \mathbf{b}, \mathbf{d}_{\ell_2}(\mathbf{x}_k)$ ; parameters  $\varepsilon_{\text{abs}}, \varepsilon_{\text{rel}}, \lambda, \rho > 0$ ,  $\gamma \in (0, 1)$ , and  $T$  (maximum inner iteration).

**Ensure:** The solution  $\mathbf{x}_{k+1}$  of the DCA subproblem.

```

1: Initialize  $\mathbf{x}_0 = \mathbf{y}_0 = \mathbf{z}_0 = \mathbf{0}$ 
2: Compute  $\eta \leftarrow 3\lambda(1 - \gamma) + \rho$ 
3: for  $t = 0$  to  $T - 1$  do
4:   if the stopping condition (4.5) is not met then
5:     Compute  $\mathbf{R}_t \leftarrow \mathbf{A}^\top \mathbf{b} + \lambda \mathbf{d}_{\ell_2}(\mathbf{x}_k) - \mathbf{y}_t + \rho \mathbf{z}_t$ 
6:     Update  $\mathbf{x}_{t+1} \leftarrow \eta^{-1} \mathbf{R}_t - \eta^{-2} \mathbf{A}^\top (\mathbf{I} + \eta^{-1} \mathbf{A} \mathbf{A}^\top)^{-1} \mathbf{A} \mathbf{R}_t$ 
7:     Update  $\mathbf{z}_{t+1} \leftarrow \mathcal{S}_{\lambda\gamma/\rho} \left( \mathbf{x}_{t+1} + \frac{1}{\rho} \mathbf{y}_t \right)$ 
8:     Update  $\mathbf{y}_{t+1} \leftarrow \mathbf{y}_t + \rho (\mathbf{x}_{t+1} - \mathbf{z}_{t+1})$ 
9:     Compute  $\varepsilon_{\text{pri}}^t, \varepsilon_{\text{dual}}^t$ , and  $\text{relerr}_t$  via (4.6)
10:   else
11:      $\mathbf{x}_{k+1} \leftarrow \mathbf{x}_t$ ; break loop
12:   end if
13: end for

```

---

their tolerances, are given by

$$(4.6a) \quad \varepsilon_{\text{pri}}^t = \sqrt{n} \varepsilon_{\text{abs}} + \varepsilon_{\text{rel}} \max(\|\mathbf{x}_t\|_2, \|\mathbf{z}_t\|_2), \quad \varepsilon_{\text{dual}}^t = \sqrt{n} \varepsilon_{\text{abs}} + \varepsilon_{\text{rel}} \|\mathbf{y}_t\|_2,$$

$$(4.6b) \quad \text{relerr}_t = \frac{\|\mathbf{x}_t - \mathbf{z}_t\|_2}{\max(\|\mathbf{x}_t\|_2, \|\mathbf{z}_t\|_2, \varepsilon)},$$

where  $\varepsilon_{\text{abs}}$  and  $\varepsilon_{\text{rel}}$  denote the absolute and relative tolerances, respectively, and  $\varepsilon$  is the machine precision. The above stopping rule follows the standard criterion proposed in [3]. ADMM for solving the DCEN-DCA subproblem is summarized in Algorithm 4.2. Since the subproblem is convex, ADMM converges to its global minimizer under standard assumptions; when embedded in DCEN-DCA (outer nonconvex loop) the whole scheme typically converges to a stationary point of the original nonconvex problem under usual DCEN-DCA assumptions [31, 20].

**4.3. Convergence analysis.** The DC decomposition in (4.1) overcomes the lack of strong convexity in the DC decomposition of the original  $\ell_1 - \ell_2$  minimization problem [40]. By introducing an additional  $\ell_2^2$  regularization term into the objective function, the function  $g(\mathbf{x})$  becomes strongly convex, and the smoothness of  $h(\mathbf{x})$  is also improved through the inclusion of the  $\ell_2^2$  regularization term. This modification not only ensures the convergence of DCEN-DCA (satisfying standard theoretical conditions) [31, 20] but also significantly enhances the well-conditioning of the subproblems and the overall robustness of the algorithm, while preserving the sparse-inducing property of the  $\ell_1 - \alpha\ell_2$  regularization. Moreover, each subproblem (4.3) admits a unique global minimizer due to its strong convexity, which further accelerates the convergence and improves the numerical stability of the iterative process.

**PROPOSITION 4.1.** *For  $\mathbf{A} \in \mathbb{R}^{m \times n}$  and  $\mathbf{b} \in \mathbb{R}^n$ , if constants  $\gamma, \alpha \in (0, 1)$  and  $\lambda > 0$ , then  $\text{argmin}_{\mathbf{x} \in \mathbb{R}^n} \mathcal{H}(\mathbf{x})$  is nonempty and compact.*

*Proof.* The function  $\mathcal{H}(\mathbf{x})$  is continuous on  $\mathbb{R}^n$  since each component term is continuous. To prove the nonemptiness, it suffices to show that  $\mathcal{H}(\mathbf{x})$  is coercive, i.e.,  $\mathcal{H}(\mathbf{x}) \rightarrow +\infty$  as  $\|\mathbf{x}\|_2 \rightarrow \infty$ . In fact, for any  $\mathbf{x} \in \mathbb{R}^n$ , since  $\|\mathbf{x}\|_1 \geq \|\mathbf{x}\|_2$  and  $\alpha \in (0, 1)$ , we have  $\|\mathbf{x}\|_1 - \alpha\|\mathbf{x}\|_2 \geq (1 - \alpha)\|\mathbf{x}\|_2$ . It follows that  $\mathcal{H}(\mathbf{x}) \geq$

$\frac{1}{2}\|\mathbf{A}\mathbf{x} - \mathbf{b}\|_2^2 + \lambda(\gamma(1 - \alpha)\|\mathbf{x}\|_2 + (1 - \gamma)\|\mathbf{x}\|_2^2) \geq \lambda(1 - \gamma)\|\mathbf{x}\|_2^2$ . For  $(1 - \gamma) > 0$ , the right-hand side tends to  $+\infty$  as  $\|\mathbf{x}\|_2 \rightarrow \infty$ , which establishes coercivity. Because  $\mathcal{H}(\mathbf{x})$  is coercive and continuous on  $\mathbb{R}^n$ , the sublevel set  $\{\mathbf{x} \in \mathbb{R}^n : \mathcal{H}(\mathbf{x}) \leq c\}$  is closed and bounded for any given constant  $c$ , and so it is compact. Thus, the solution set  $\operatorname{argmin}_{\mathbf{x} \in \mathbb{R}^n} \mathcal{H}(\mathbf{x})$  is nonempty and compact.  $\square$

*Remark 4.2.* It is worth noting that the existence result in Proposition 4.1 does not require any specific assumptions on the matrix  $\mathbf{A}$  or the vector  $\mathbf{b}$ . Even if  $\mathbf{A}$  is rank-deficient or  $\mathbf{A} = \mathbf{0}$ , the coercivity of  $\mathcal{H}(\mathbf{x})$  is guaranteed by the quadratic term  $\lambda(1 - \gamma)\|\mathbf{x}\|_2^2$ , which ensures that  $\mathcal{H}(\mathbf{x}) \rightarrow +\infty$  as  $\|\mathbf{x}\|_2 \rightarrow \infty$ . However, when  $\gamma = 1$  and  $\alpha > 1$  [24], the quadratic term vanishes and  $\mathcal{H}(\mathbf{x})$  may lose coercivity, in which case additional assumptions on  $\mathbf{A}$ ,  $\mathbf{b}$ , and constants  $\lambda$  and  $\alpha$  are required to guarantee the existence of a minimizer.

**LEMMA 4.3.** *Let  $\mathbf{A} \in \mathbb{R}^{m \times n}$ ,  $\mathbf{b} \in \mathbb{R}^m$  with  $\mathbf{b} \neq \mathbf{0}$ ,  $\lambda > 0$ ,  $\gamma \in (0, 1)$ , and  $\alpha \in (0, 1)$ . If  $\mathbf{b} \notin \operatorname{ker}(\mathbf{A}^\top)$  and*

$$(4.7) \quad \|\mathbf{A}^\top \mathbf{b}\|_2 > \lambda\gamma(\sqrt{n} + \alpha),$$

*then  $\mathbf{x} = \mathbf{0}$  is not a stationary point of DCEN.*

*Proof.* Assume, for contradiction, that  $\mathbf{x} = \mathbf{0}$  is a stationary point. Since the objective function  $\mathcal{H}(\mathbf{x})$  is proper and lower semicontinuous, a necessary condition for optimality is that  $\mathbf{0} \in \partial\mathcal{H}(\mathbf{0})$ . The subdifferential of  $\mathcal{H}(\mathbf{x})$  at  $\mathbf{0}$  is given by  $\partial\mathcal{H}(\mathbf{0}) = -\mathbf{A}^\top \mathbf{b} + \lambda\gamma(\partial\|\cdot\|_1(\mathbf{0}) - \alpha\partial\|\cdot\|_2(\mathbf{0}))$ . Recall that  $\partial\|\cdot\|_1(\mathbf{0}) = \{\mathbf{u} \in \mathbb{R}^n : \|\mathbf{u}\|_\infty \leq 1\}$ ,  $\partial\|\cdot\|_2(\mathbf{0}) = \{\mathbf{v} \in \mathbb{R}^n : \|\mathbf{v}\|_2 \leq 1\}$ . Thus,  $\mathbf{0} \in \partial\mathcal{H}(\mathbf{0})$  implies the existence of  $\mathbf{u}$  and  $\mathbf{v}$  satisfying  $\|\mathbf{u}\|_\infty \leq 1$  and  $\|\mathbf{v}\|_2 \leq 1$  such that  $\mathbf{A}^\top \mathbf{b} = \lambda\gamma(\mathbf{u} - \alpha\mathbf{v})$ . Taking the Euclidean norm of both sides and applying the triangle inequality yields  $\|\mathbf{A}^\top \mathbf{b}\|_2 \leq \lambda\gamma(\|\mathbf{u}\|_2 + \alpha\|\mathbf{v}\|_2) \leq \lambda\gamma(\sqrt{n}\|\mathbf{u}\|_\infty + \alpha \cdot 1) \leq \lambda\gamma(\sqrt{n} + \alpha)$ . This contradicts the assumption (4.7). Therefore,  $\mathbf{0}$  cannot be a stationary point.  $\square$

Lemma 4.3 indicates that, in most practical scenarios, the optimal solution of DCEN is nonzero. Indeed, condition (4.7) is typically satisfied when the regularization parameter  $\lambda$  is small, which is the usual case in sparse learning and signal recovery applications. Only when a strong regularization is imposed, i.e., when  $\lambda$  takes a sufficiently large value, the zero vector may be a potential minimizer.

**THEOREM 4.4** (Sufficient descent). *Let  $\{\mathbf{x}_k\}$  be the sequence generated by the iteration framework (4.2) and parameters  $\lambda > 0$ ,  $\alpha \in (0, 1)$ , and  $\gamma \in (0, 1)$ . Define  $\mu_g := \lambda_{\min}(\mathbf{A}^\top \mathbf{A}) + 3\lambda(1 - \gamma) > 0$  and  $c := \frac{\mu_g}{2}$ . Then, the sequence  $\{\mathbf{x}_k\}$  satisfies the sufficient decrease property*

$$(4.8) \quad \mathcal{H}(\mathbf{x}_k) - \mathcal{H}(\mathbf{x}_{k+1}) \geq c\|\mathbf{x}_k - \mathbf{x}_{k+1}\|_2^2.$$

*Proof.* The function  $g_{\text{quad}}(\mathbf{x}) = \frac{1}{2}\|\mathbf{A}\mathbf{x} - \mathbf{b}\|_2^2 + \frac{3\lambda(1-\gamma)}{2}\|\mathbf{x}\|_2^2$  has Hessian matrix  $\nabla^2 g_{\text{quad}}(\mathbf{x}) = \mathbf{A}^\top \mathbf{A} + 3\lambda(1 - \gamma)\mathbf{I} \succ 0$ , implying that  $g_{\text{quad}}$  is  $\mu_g$ -strongly convex. Since  $\lambda\gamma\|\mathbf{x}\|_1$  is convex, we know that  $g$  is  $\mu_g$ -strongly convex. Hence, for any  $\mathbf{x}, \mathbf{y} \in \mathbb{R}^n$  and  $\mathbf{s} \in \partial g(\mathbf{y})$ , one has

$$(4.9) \quad g(\mathbf{x}) \geq g(\mathbf{y}) + \langle \mathbf{s}, \mathbf{x} - \mathbf{y} \rangle + \frac{\mu_g}{2}\|\mathbf{x} - \mathbf{y}\|_2^2.$$

For  $\mathbf{y} \neq 0$ , the subdifferential of  $h$  satisfies  $\partial h(\mathbf{y}) = \lambda(\alpha\gamma\mathbf{y}/\|\mathbf{y}\|_2 + (1 - \gamma)\mathbf{y}) = \lambda\mathbf{d}_{\ell_2}(\mathbf{y})$ . It follows from the convexity of  $h$  that

$$(4.10) \quad h(\mathbf{y}) \geq h(\mathbf{x}) + \langle \mathbf{s}, \mathbf{y} - \mathbf{x} \rangle, \quad \forall \mathbf{s} \in \partial h(\mathbf{x}).$$

When  $\mathbf{x}_k \neq 0$ , the optimality condition of DCEN-DCA subproblem gives  $\mathbf{0} \in \partial g(\mathbf{x}_{k+1}) - \lambda \mathbf{d}_{\ell_2}(\mathbf{x}_k)$ , that is,  $\mathbf{s}_g := \lambda \mathbf{d}_{\ell_2}(\mathbf{x}_k) \in \partial g(\mathbf{x}_{k+1})$ . Applying (4.9) with  $\mathbf{x} = \mathbf{x}_k$ ,  $\mathbf{y} = \mathbf{x}_{k+1}$ , and  $\mathbf{s} = \mathbf{s}_g$  yields

$$(4.11) \quad g(\mathbf{x}_k) - g(\mathbf{x}_{k+1}) \geq \lambda \langle \mathbf{d}_{\ell_2}(\mathbf{x}_k), \mathbf{x}_k - \mathbf{x}_{k+1} \rangle + \frac{\mu_g}{2} \|\mathbf{x}_k - \mathbf{x}_{k+1}\|_2^2.$$

By (4.10), taking  $\mathbf{x} = \mathbf{x}_k$ ,  $\mathbf{y} = \mathbf{x}_{k+1}$ , and  $\mathbf{s} = \lambda \mathbf{d}_{\ell_2}(\mathbf{x}_k) \in \partial h(\mathbf{x}_k)$  gives

$$(4.12) \quad h(\mathbf{x}_k) - h(\mathbf{x}_{k+1}) \leq \lambda \langle \mathbf{d}_{\ell_2}(\mathbf{x}_k), \mathbf{x}_k - \mathbf{x}_{k+1} \rangle.$$

Substituting (4.11) and (4.12) into  $\mathcal{H}(\mathbf{x}_k) - \mathcal{H}(\mathbf{x}_{k+1}) = [g(\mathbf{x}_k) - g(\mathbf{x}_{k+1})] - [h(\mathbf{x}_k) - h(\mathbf{x}_{k+1})]$ , we obtain

$$\begin{aligned} \mathcal{H}(\mathbf{x}_k) - \mathcal{H}(\mathbf{x}_{k+1}) &\geq \left( \lambda \langle \mathbf{d}_{\ell_2}(\mathbf{x}_k), \mathbf{x}_k - \mathbf{x}_{k+1} \rangle + \frac{\mu_g}{2} \|\mathbf{x}_k - \mathbf{x}_{k+1}\|_2^2 \right) \\ &\quad - \lambda \langle \mathbf{d}_{\ell_2}(\mathbf{x}_k), \mathbf{x}_k - \mathbf{x}_{k+1} \rangle = \frac{\mu_g}{2} \|\mathbf{x}_k - \mathbf{x}_{k+1}\|_2^2. \end{aligned}$$

When  $\mathbf{x}_k = \mathbf{0}$ , the subproblem of DCEN-DCA reduces to  $\mathbf{x}_{k+1} = \arg \min g(\mathbf{x})$ , implying  $\mathbf{0} \in \partial g(\mathbf{x}_{k+1})$ . Applying (4.9) with  $\mathbf{x} = \mathbf{0}$ ,  $\mathbf{y} = \mathbf{x}_{k+1}$ , and  $\mathbf{s} = \mathbf{0}$  gives

$$\begin{aligned} \mathcal{H}(\mathbf{0}) - \mathcal{H}(\mathbf{x}_{k+1}) &\geq g(\mathbf{0}) - g(\mathbf{x}_{k+1}) \quad (\text{since } h(\mathbf{x}_{k+1}) \geq 0) \\ &\stackrel{(4.9)}{\geq} \frac{\mu_g}{2} \|\mathbf{x}_{k+1}\|_2^2 = \frac{\mu_g}{2} \|\mathbf{x}_k - \mathbf{x}_{k+1}\|_2^2. \end{aligned}$$

Thus, when  $\mathbf{x}_k = \mathbf{0}$ , one has  $\mathcal{H}(\mathbf{x}_k) - \mathcal{H}(\mathbf{x}_{k+1}) \geq \frac{\mu_g}{2} \|\mathbf{x}_k - \mathbf{x}_{k+1}\|_2^2$ .  $\square$

**THEOREM 4.5.** *Let  $\{\mathbf{x}_k\}$  be the sequence generated by the iteration scheme (4.2) with parameters  $\lambda > 0$ ,  $\alpha \in (0, 1)$ , and  $\gamma \in (0, 1)$ . Then the following statements hold:*

- (a)  $\{\mathbf{x}_k\}$  is bounded;
- (b)  $\|\mathbf{x}_{k+1} - \mathbf{x}_k\|_2 \rightarrow 0$  as  $k \rightarrow \infty$ ;
- (c) Every limit point  $\mathbf{x}^*$  of  $\{\mathbf{x}_k\}$  satisfies  $\mathbf{0} \in \partial \mathcal{H}(\mathbf{x}^*)$ .

*Proof.* (a) By the coercivity of  $\mathcal{H}$  established in Proposition 4.1 and  $\mathcal{H}(\mathbf{x}_{k+1}) \leq \mathcal{H}(\mathbf{x}_k) \leq \mathcal{H}(\mathbf{x}_0)$  for any  $k \geq 0$ , it follows that the sequence  $\mathbf{x}_k$  is bounded.

(b) By the sufficient decrease property (4.8) and Lemma 4.1, we have  $\mathcal{H}(\mathbf{x}_{k+1}) \leq \mathcal{H}(\mathbf{x}_k)$  for all  $k \geq 0$  and  $\{\mathcal{H}(\mathbf{x}_k)\}$  admits a finite infimum  $\underline{\mathcal{H}} := \inf_{\mathbf{x} \in \mathbb{R}^n} \mathcal{H}(\mathbf{x}) > -\infty$ . It follows that the monotone sequence  $\{\mathcal{H}(\mathbf{x}_k)\}$  is bounded below and convergent. Denote its limit by  $\mathcal{H}_\infty$ . Sum (4.8) for  $k = 0, 1, \dots, K-1$  to obtain the telescoping inequality  $\mathcal{H}(\mathbf{x}_0) - \mathcal{H}(\mathbf{x}_K) \geq c \sum_{k=0}^{K-1} \|\mathbf{x}_k - \mathbf{x}_{k+1}\|_2^2$ . Since  $\mathcal{H}(\mathbf{x}_K) \downarrow \mathcal{H}_\infty$  and  $\mathcal{H}(\mathbf{x}_0) - \mathcal{H}_\infty < +\infty$ , it follows that  $\sum_{k=0}^{\infty} \|\mathbf{x}_k - \mathbf{x}_{k+1}\|_2^2 \leq \frac{1}{c} (\mathcal{H}(\mathbf{x}_0) - \mathcal{H}_\infty) < +\infty$ , which implies  $\lim_{k \rightarrow \infty} \|\mathbf{x}_k - \mathbf{x}_{k+1}\|_2^2 = 0$  and so  $\|\mathbf{x}_k - \mathbf{x}_{k+1}\|_2 \rightarrow 0$ .

(c) Let  $\mathbf{x}^*$  be a limit point of the sequence  $\{\mathbf{x}_k\}$  generated by DCEN-DCA. Then there exists a subsequence  $\{\mathbf{x}_{k_j}\}$  such that  $\mathbf{x}_{k_j} \rightarrow \mathbf{x}^*$  as  $j \rightarrow \infty$ . Since  $\|\mathbf{x}_{k+1} - \mathbf{x}_k\|_2 \rightarrow 0$ , it follows that  $\mathbf{x}_{k_j+1} \rightarrow \mathbf{x}^*$ . From the optimality condition of subproblem (4.3), for each  $k$ , there exists  $\mathbf{s}_k \in \partial h(\mathbf{x}_k)$  such that  $\mathbf{s}_k \in \partial g(\mathbf{x}_{k+1})$ . Since  $\{\mathbf{x}_{k_j}\}$  and  $\{\mathbf{x}_{k_j+1}\}$  are bounded and both  $g$  and  $h$  are proper, lower semicontinuous, and convex, the subdifferentials  $\partial h$  and  $\partial g$  are locally bounded [28, Theorem 24.7]. Hence, the sequence  $\{\mathbf{s}_{k_j}\}$  is bounded and admits a convergent subsequence (still denoted  $\{\mathbf{s}_{k_j}\}$ ) with limit  $\mathbf{s}^* \in \mathbb{R}^n$ . Because  $\partial h$  and  $\partial g$  have closed graphs [28, Theorem 24.4], the convergences  $\mathbf{x}_{k_j} \rightarrow \mathbf{x}^*$ ,  $\mathbf{x}_{k_j+1} \rightarrow \mathbf{x}^*$ , and  $\mathbf{s}_{k_j} \rightarrow \mathbf{s}^*$ , together with the inclusions  $\mathbf{s}_{k_j} \in \partial h(\mathbf{x}_{k_j})$  and  $\mathbf{s}_{k_j} \in \partial g(\mathbf{x}_{k_j+1})$ , imply that  $\mathbf{s}^* \in \partial h(\mathbf{x}^*)$  and  $\mathbf{s}^* \in \partial g(\mathbf{x}^*)$ . Thus,  $\mathbf{0} \in \partial g(\mathbf{x}^*) - \partial h(\mathbf{x}^*) = \partial \mathcal{H}(\mathbf{x}^*)$  and so  $\mathbf{x}^*$  is a stationary point of  $\mathcal{H}$ .  $\square$

**4.4. Global convergence and convergence rate.** This subsection presents the global convergence analysis of DCEN-DCA. We first show that the sequence  $\{\mathbf{x}^t\}$  generated by DCEN-DCA is convergent to a stationary point of  $\mathcal{H}$  under mild assumptions. Our analysis follows the work due to [30, 41, 2, 36].

**PROPOSITION 4.6.** *Let  $\{\mathbf{x}_k\}$  be the sequence generated by DCEN-DCA for minimizing  $\mathcal{H}(\mathbf{x})$ . Then the following statements hold:*

- (a) *The limit  $\lim_{k \rightarrow \infty} \mathcal{H}(\mathbf{x}_k) = \zeta$  exists;*
- (b) *For any  $\hat{\mathbf{x}} \in \mathcal{A}$ ,  $\mathcal{H}(\hat{\mathbf{x}}) = \zeta$ , where  $\mathcal{A}$  is the set of accumulation points of the sequence  $\{\mathbf{x}_k\}$ .*

*Proof.* (a) By Theorem 4.4 and Proposition 4.1,  $\mathcal{H}(\mathbf{x}_k)$  is non-increasing and  $\mathcal{H}$  is level-bounded. It follows that the limit  $\lim_{k \rightarrow \infty} \mathcal{H}(\mathbf{x}_k) = \zeta$  exists.

(b) The update rule of DCEN-DCA states that at each iteration  $k$ , there exists a subgradient  $\xi_k \in \partial h(\mathbf{x}_k)$  such that  $\mathbf{x}_{k+1} \in \arg \min_{\mathbf{x} \in \mathbb{R}^n} \{g(\mathbf{x}) - \langle \xi_k, \mathbf{x} \rangle\}$ , which implies  $\xi_k \in \partial g(\mathbf{x}_{k+1})$ . Let  $\hat{\mathbf{x}} \in \mathcal{A}$  be an arbitrary accumulation point. Then there is a subsequence  $\{\mathbf{x}_{k_i}\}$  such that  $\lim_{i \rightarrow \infty} \mathbf{x}_{k_i} = \hat{\mathbf{x}}$ . For any  $\hat{\mathbf{z}} \in \mathbb{R}^n$ , we have  $g(\mathbf{x}_{k_i+1}) - \langle \xi_{k_i}, \mathbf{x}_{k_i+1} \rangle \leq g(\hat{\mathbf{z}}) - \langle \xi_{k_i}, \hat{\mathbf{z}} \rangle$ . Choosing  $\hat{\mathbf{z}} = \hat{\mathbf{x}}$  and rearranging yield

$$(4.13) \quad g(\mathbf{x}_{k_i+1}) \leq g(\hat{\mathbf{x}}) + \langle \xi_{k_i}, \mathbf{x}_{k_i+1} - \hat{\mathbf{x}} \rangle.$$

Since  $\{\mathbf{x}_{k_i}\}$  and  $\{\mathbf{x}_{k_i+1}\}$  are contained in the compact level set  $\mathcal{S}_{\mathcal{H}} = \{\mathbf{x} : \mathcal{H}(\mathbf{x}) \leq \mathcal{H}(\mathbf{x}_0)\}$  and  $h$  is convex and continuous on  $\mathbb{R}^n$ ,  $\partial h$  is bounded on  $\mathcal{S}_{\mathcal{H}}$ . Consequently, the sequence of subgradients  $\{\xi_{k_i}\}$  is bounded, and thus possesses a convergent subsequence, denotes it again by  $\{\xi_{k_i}\}$ , such that  $\xi_{k_i} \rightarrow \xi^*$  for some  $\xi^* \in \mathbb{R}^n$ . Using (4.13), one has  $\zeta = \lim_{i \rightarrow \infty} \mathcal{H}(\mathbf{x}_{k_i+1}) \leq \limsup_{i \rightarrow \infty} [g(\hat{\mathbf{x}}) - h(\mathbf{x}_{k_i+1}) + \langle \xi_{k_i}, \mathbf{x}_{k_i+1} - \hat{\mathbf{x}} \rangle]$ . By the continuity of  $g$  and  $h$ , the term  $\langle \xi_{k_i}, \mathbf{x}_{k_i+1} - \hat{\mathbf{x}} \rangle$  converges to 0. Therefore, the right-hand side equals  $g(\hat{\mathbf{x}}) - h(\hat{\mathbf{x}}) = \mathcal{H}(\hat{\mathbf{x}})$ , establishing  $\zeta \leq \mathcal{H}(\hat{\mathbf{x}})$ . On the other hand, since  $\mathcal{H}$  is the difference of a continuous function  $g$  and a lower semicontinuous function  $h$ , it is lower semicontinuous. Thus,  $\mathcal{H}(\hat{\mathbf{x}}) \leq \liminf_{i \rightarrow \infty} \mathcal{H}(\mathbf{x}_{k_i}) = \zeta$  and so  $\mathcal{H}(\hat{\mathbf{x}}) = \zeta$ . As  $\hat{\mathbf{x}}$  was chosen arbitrarily from  $\mathcal{A}$ , the proof is complete.  $\square$

**DEFINITION 4.7 (KL property).** *Let  $\mathcal{P}$  be a proper closed function and  $\mathbf{x} \in \text{dom } \partial \mathcal{P}$ . We say that  $\mathcal{P}$  satisfies the KL property at  $\mathbf{x}$  if there exist  $p \in (0, +\infty]$ , a neighborhood  $\mathcal{O}$  of  $\mathbf{x}$ , and a concave function  $\phi : [0, p) \rightarrow \mathbb{R}_+$  with  $\phi(0) = 0$ ,  $\phi \in C^1(0, p)$  and  $\phi' > 0$ , such that  $\phi'(\mathcal{P}(\hat{\mathbf{x}}) - \mathcal{P}(\mathbf{x})) \text{dist}(0, \partial \mathcal{P}(\hat{\mathbf{x}})) \geq 1$ , for all  $\hat{\mathbf{x}} \in \mathcal{O}$  satisfying  $\mathcal{P}(\mathbf{x}) < \mathcal{P}(\hat{\mathbf{x}}) < \mathcal{P}(\mathbf{x}) + p$ .*

If  $\mathcal{P}$  satisfies the KL property at every point in  $\text{dom } \partial \mathcal{P}$ , then  $\mathcal{P}$  is called a KL function.

**LEMMA 4.8 (Uniformized KL property [1]).** *Suppose that  $\mathcal{P}$  is a proper closed function and let  $\Theta$  be a compact set on which  $\mathcal{P}$  is constant. If  $\mathcal{P}$  satisfies the KL property at every point of  $\Theta$ , then there exist constants  $\varepsilon, p > 0$  and a function  $\phi \in \Phi_p$  such that  $\phi'(\mathcal{P}(\hat{\mathbf{x}}) - \mathcal{P}(\mathbf{x})) \text{dist}(0, \partial \mathcal{P}(\hat{\mathbf{x}})) \geq 1$ , for all  $\hat{\mathbf{x}} \in \Theta$  and all  $\mathbf{x}$  satisfying  $\text{dist}(\mathbf{x}, \Theta) < \varepsilon$  and  $\mathcal{P}(\hat{\mathbf{x}}) < \mathcal{P}(\mathbf{x}) < \mathcal{P}(\hat{\mathbf{x}}) + p$ , where  $\Phi_p$  denotes the class of concave continuous functions  $\phi : [0, p) \rightarrow \mathbb{R}_+$  with  $\phi(0) = 0$  that are continuously differentiable on  $(0, p)$  and satisfy  $\phi' > 0$ .*

Let  $\mathcal{B}_\epsilon(\mathbf{0}) = \{\mathbf{x} : \|\mathbf{x}\|_2 \leq \epsilon\} \subset \mathbb{R}^n$  be the closed ball of radius  $\epsilon > 0$  centered at the origin, and let  $\text{crit}(\mathcal{H})$  denote the set of all critical points of  $\mathcal{H}$ . We now establish the global convergence of DCEN-DCA.

**THEOREM 4.9 (Global convergence of DCEN-DCA).** *Let the sequence  $\{\mathbf{x}_k\}$  be generated by DCEN-DCA. For parameters  $\alpha \in (0, 1)$ ,  $\lambda > 0$ , and  $\gamma \in (0, 1)$ , if the*

subgradients of  $g$  and  $h$  at  $\mathbf{0}$  satisfy  $(-\mathbf{A}^\top \mathbf{b} + \partial(\lambda\gamma\|\cdot\|_1)(\mathbf{0})) \cap \partial(\lambda\alpha\gamma\|\cdot\|_2)(\mathbf{0}) = \emptyset$ , then the following statements hold:

- (a)  $\lim_{k \rightarrow \infty} \text{dist}(\mathbf{0}, \partial\mathcal{H}(\mathbf{x}_k)) = 0$ ;
- (b) The sequence  $\{\mathbf{x}_k\}$  converges to a stationary point of  $\mathcal{H}$  and  $\sum_{k=1}^{\infty} \|\mathbf{x}_k - \mathbf{x}_{k-1}\|_2 < \infty$ .

*Proof.* (a) As  $\mathcal{H}$  is bounded below, the sequence  $\{\mathbf{x}_k\}$  is bounded and its set of accumulation points  $\mathcal{A}$  is nonempty and compact. The assumption that  $\partial g(\mathbf{0}) \cap \partial h(\mathbf{0}) = \emptyset$  implies that  $\mathbf{0}$  is not a stationary point of  $\mathcal{H}$ . By Theorem 4.5, no accumulation point of  $\{\mathbf{x}_k\}$  can be  $\mathbf{0}$ . Consequently, there exists a sufficiently small  $\epsilon > 0$  such that  $\mathcal{A} \subseteq \text{crit}(\mathcal{H}) \subseteq B_\epsilon^c(\mathbf{0}) := \{\mathbf{x} \in \mathbb{R}^n : \|\mathbf{x}\|_2 > \epsilon\}$ . Thus, for any  $\delta > 0$ , there is  $K_0 > 0$  such that  $\text{dist}(\mathbf{x}_k, \mathcal{A}) < \delta$  and  $\mathbf{x}_k \in B_\epsilon^c(\mathbf{0})$  for all  $k > K_0$ , and so  $\mathcal{H}$  is Lipschitz continuously differentiable on the open set  $B_\epsilon^c(\mathbf{0})$ . The optimality condition of (4.3) yields  $\nabla h(\mathbf{x}_{k-1}) \in \partial g(\mathbf{x}_k)$ . Since  $g$  is convex and  $h$  is continuously differentiable on  $B_\epsilon^c(\mathbf{0})$ , one has  $\partial\mathcal{H}(\mathbf{x}_k) = \partial g(\mathbf{x}_k) - \nabla h(\mathbf{x}_k)$  and so  $\nabla h(\mathbf{x}_{k-1}) - \nabla h(\mathbf{x}_k) \in \partial\mathcal{H}(\mathbf{x}_k)$ , which implies  $\text{dist}(\mathbf{0}, \partial\mathcal{H}(\mathbf{x}_k)) \leq \|\nabla h(\mathbf{x}_{k-1}) - \nabla h(\mathbf{x}_k)\|_2$ . Since  $\nabla h$  is Lipschitz continuous on  $B_\epsilon^c(\mathbf{0})$  with the Lipschitz constant  $L_h = \lambda(\frac{\alpha\gamma}{\epsilon} + 1 - \gamma) > 0$ , we have  $\text{dist}(\mathbf{0}, \partial\mathcal{H}(\mathbf{x}_k)) \leq L_h \|\mathbf{x}_k - \mathbf{x}_{k-1}\|_2$ .

(b) By part (c) of Theorem 4.5, it suffices to establish the convergence of the sequence  $\{\mathbf{x}_k\}$ . If there exists  $k_0 \geq 1$  such that  $\mathcal{H}(\mathbf{x}_{k_0}) = \zeta$ , then the sequence  $\{\mathbf{x}_k\}$  converges in finitely many steps. Hence, we assume, without loss of generality, that  $\mathcal{H}(\mathbf{x}_k) > \zeta$  for all  $k \geq 1$ . Since  $\mathcal{H}$  is a KL function on the open set  $B_\epsilon^c(\mathbf{0})$ , Lemma 4.8 and Proposition 4.6 guarantee that there are  $\tilde{\epsilon} > 0$ ,  $\sigma > 0$ , and a continuous concave function  $\phi \in \Phi_\sigma$  such that the KL inequality  $\phi'(\mathcal{H}(\mathbf{x}) - \zeta) \cdot \text{dist}(\mathbf{0}, \partial\mathcal{H}(\mathbf{x})) \geq 1$  holds for all  $\mathbf{x} \in \mathcal{U}$ , where  $\mathcal{U} := \{\mathbf{x} \in B_\epsilon^c(\mathbf{0}) : \text{dist}(\mathbf{x}, \mathcal{A}) < \tilde{\epsilon}\} \cap \{\mathbf{x} \in B_\epsilon^c(\mathbf{0}) : \zeta < \mathcal{H}(\mathbf{x}) < \zeta + \sigma\}$ . Since  $\mathcal{A}$  is the set of accumulation points of  $\{\mathbf{x}_k\}$  and  $\{\mathbf{x}_k\}$  is bounded, there exists  $K_1 > 0$  such that  $\text{dist}(\mathbf{x}_k, \mathcal{A}) < \tilde{\epsilon}$  for all  $k > K_1$ . Moreover, since  $\mathcal{H}(\mathbf{x}_k) \rightarrow \zeta$ , there exists  $K_2 > 0$  such that  $\zeta < \mathcal{H}(\mathbf{x}_k) < \zeta + \sigma$  for all  $k > K_2$ . Letting  $\tilde{K} := \max\{K_0 + 1, K_1, K_2\}$ , we conclude that  $\mathbf{x}_k \in \mathcal{U}$  for all  $k > \tilde{K}$ . Thus, one has  $\phi'(\mathcal{H}(\mathbf{x}_k) - \zeta) \cdot \text{dist}(\mathbf{0}, \partial\mathcal{H}(\mathbf{x}_k)) \geq 1$ , for any  $k > \tilde{K}$ . Using the concavity of  $\phi$  and Theorem 4.4, we have

$$\begin{aligned} \frac{\mu_g}{2} \|\mathbf{x}_k - \mathbf{x}_{k-1}\|_2^2 &\leq [\phi(\mathcal{H}(\mathbf{x}_{k-1}) - \zeta) - \phi(\mathcal{H}(\mathbf{x}_k) - \zeta)] \cdot \text{dist}(\mathbf{0}, \partial\mathcal{H}(\mathbf{x}_k)) \\ &\leq [\phi(\mathcal{H}(\mathbf{x}_{k-1}) - \zeta) - \phi(\mathcal{H}(\mathbf{x}_k) - \zeta)] \cdot L_h \|\mathbf{x}_k - \mathbf{x}_{k-1}\|_2, \quad \forall k > \tilde{K}. \end{aligned}$$

Rearranging the above inequality yields

$$(4.14) \quad \|\mathbf{x}_k - \mathbf{x}_{k-1}\|_2 \leq \frac{2L_h}{\mu_g} [\phi(\mathcal{H}(\mathbf{x}_{k-1}) - \zeta) - \phi(\mathcal{H}(\mathbf{x}_k) - \zeta)].$$

Summing the inequality (4.14) from  $k = \tilde{K}$  to  $\infty$  and noting that  $\phi \geq 0$ , we obtain  $\sum_{k=\tilde{K}}^{\infty} \|\mathbf{x}_k - \mathbf{x}_{k-1}\|_2 \leq \frac{2L_h}{\mu_g} \phi(\mathcal{H}(\mathbf{x}_{\tilde{K}}) - \zeta) < \infty$  and so  $\sum_{k=0}^{\infty} \|\mathbf{x}_k - \mathbf{x}_{k-1}\|_2 < \infty$ .  $\square$

**THEOREM 4.10.** Let  $\{\mathbf{x}_k\}$  be the sequence generated by DCEN-DCA. Define  $\Lambda^* := \text{supp}(\mathbf{x}^*)$  and  $\Xi := \{\mathbf{x} \in \mathbb{R}^n \mid \text{supp}(\mathbf{x}) = \Lambda^*, \text{sign}(\mathbf{x}) = \text{sign}(\mathbf{x}^*)\}$ . For parameters  $\alpha \in (0, 1)$ ,  $\lambda > 0$ , and  $\gamma \in (0, 1)$ , if  $\mathbf{b} \notin \ker(\mathbf{A}^\top)$  and  $\|\mathbf{A}^\top \mathbf{b}\|_2 > \lambda\gamma(\sqrt{n} + \alpha)$ , then the following statements hold:

- (a) There exists an index  $K$  such that  $\mathbf{x}_k \in \Xi$  when  $k \geq K$ ;
- (b) If the desingularizing function in the KL inequality in Definition 4.7 is given by  $\phi(v) = Cv^{1-\theta}$  for some  $\theta \in [0, 1)$  and  $C > 0$ , then there exist  $\tilde{\gamma} > 0$

and  $\epsilon > 0$  such that  $\{\mathbf{x}_k\}$  converges linearly when  $0 < \gamma < \tilde{\gamma}$  and  $\lambda\alpha > \epsilon\sigma_{\min}(\mathbf{A}_{\Lambda^*}^\top \mathbf{A}_{\Lambda^*})$ , i.e., there exist  $q > 0$  and  $\omega \in (0, 1)$  such that  $\|\mathbf{x}_k - \mathbf{x}_*\|_2 \leq q\omega^k$ .

*Proof.* (a) Let  $\Lambda^* = \text{supp}(\mathbf{x}^*)$  and  $\omega = \min_{i \in \Lambda^*} |x_i^*| > 0$ . Suppose, for contradiction, that  $\text{supp}(\mathbf{x}_k)$  is not eventually equal to  $\Lambda^*$ . Then there exists a subsequence with constant support  $\Lambda \neq \Lambda^*$ . Since this subsequence also converges to  $\mathbf{x}^*$ , we must have  $\Lambda^* = \Lambda$ , a contradiction. Thus,  $\text{supp}(\mathbf{x}_k) = \Lambda^*$  for all sufficiently large  $k$ . Since  $\mathbf{x}_k \rightarrow \mathbf{x}^*$ , there exists  $K$  such that  $\|\mathbf{x}_k - \mathbf{x}^*\|_2 < \omega$  whenever  $k \geq K$ . For any  $i \in \Lambda^*$ ,  $|(\mathbf{x}_k)_i - x_i^*| \leq \|\mathbf{x}_k - \mathbf{x}^*\|_2 < \omega \leq |x_i^*|$ , which implies  $\text{sign}((\mathbf{x}_k)_i) = \text{sign}(x_i^*)$ . It follows that  $\mathbf{x}_k \in \Xi$  for all  $k \geq K$ .

(b) To demonstrate that the function  $\mathcal{H}$  restricted to the set  $\Xi$  satisfies the KL property with exponent  $\frac{1}{2}$ , we introduce an auxiliary function  $\widehat{\mathcal{H}} : \mathbb{R}^{|\Lambda^*|} \rightarrow \mathbb{R}$ , defined as  $\widehat{\mathcal{H}}(\mathbf{u}) = \frac{1}{2}\|\mathbf{A}_{\Lambda^*}\mathbf{u} - \mathbf{b}\|_2^2 + \lambda(\gamma\|\mathbf{u}\|_1 + (1-\gamma)\|\mathbf{u}\|_2^2) - \lambda\gamma\alpha\|\mathbf{u}\|_2$ . Observe that for any  $\mathbf{x} \in \Xi$ , it holds that  $\widehat{\mathcal{H}}(\mathbf{x}_{\Lambda^*}) = H(\mathbf{x})$ . Define the set  $\Xi_{\Lambda^*} := \{\mathbf{u} \in \mathbb{R}^{|\Lambda^*|} \mid \mathbf{u} = \mathbf{x}_{\Lambda^*}, \mathbf{x} \in \Xi\}$ . Then  $\widehat{\mathcal{H}}$  is continuously differentiable on  $\Xi_{\Lambda^*}$  and  $\nabla \widehat{\mathcal{H}}(\mathbf{u}) = \mathbf{A}_{\Lambda^*}^\top (\mathbf{A}_{\Lambda^*}\mathbf{u} - \mathbf{b}) + 2\lambda(1-\gamma)\mathbf{u} + \lambda\gamma\text{sign}(\mathbf{u}) - \lambda\gamma\alpha \frac{\mathbf{u}}{\|\mathbf{u}\|_2}$  for all  $\mathbf{u} \in \Xi_{\Lambda^*}$ . Let  $\epsilon < \omega$ . Then it is evident that  $\mathbf{x}^* \in B_\epsilon^c(\mathbf{0})$ . Next, we verify the inequality  $\|\nabla \widehat{\mathcal{H}}(\mathbf{x}_{\Lambda^*}) - \nabla \widehat{\mathcal{H}}(\mathbf{x}_{\Lambda^*}^*)\|_2 \geq \tau\|\mathbf{x}_{\Lambda^*} - \mathbf{x}_{\Lambda^*}^*\|_2$  for all  $\mathbf{x} \in \Xi \cap B_\epsilon^c(\mathbf{0})$ , where  $\tau > 0$ . Indeed, let  $B_\epsilon^c(\mathbf{0})_{\Lambda^*} := \{\mathbf{u} \in \mathbb{R}^{|\Lambda^*|} \mid \mathbf{u} = \mathbf{x}_{\Lambda^*}, \mathbf{x} \in B_\epsilon^c(\mathbf{0})\}$ . Then for any  $\mathbf{u}, \mathbf{v} \in \Xi_{\Lambda^*} \cap B_\epsilon^c(\mathbf{0})_{\Lambda^*}$ , we have  $\left\| \frac{\mathbf{u}}{\|\mathbf{u}\|_2} - \frac{\mathbf{v}}{\|\mathbf{v}\|_2} \right\|_2^2 = \frac{1}{\|\mathbf{u}\|_2\|\mathbf{v}\|_2} (2\|\mathbf{u}\|_2\|\mathbf{v}\|_2 - 2\langle \mathbf{u}, \mathbf{v} \rangle) \leq \frac{1}{\|\mathbf{u}\|_2\|\mathbf{v}\|_2} \|\mathbf{u} - \mathbf{v}\|_2^2$ . Set  $\hat{L} = \frac{1}{\epsilon}$ . Since  $\|\mathbf{u}\|_2 \geq \epsilon$  and  $\|\mathbf{v}\|_2 \geq \epsilon$ , it follows that  $\left\| \frac{\mathbf{u}}{\|\mathbf{u}\|_2} - \frac{\mathbf{v}}{\|\mathbf{v}\|_2} \right\|_2 \leq \frac{1}{\epsilon} \|\mathbf{u} - \mathbf{v}\|_2 = \hat{L} \|\mathbf{u} - \mathbf{v}\|_2$ . For any  $\mathbf{x} \in \Xi \cap B_\epsilon^c(\mathbf{0})$ , we have

$$(4.15) \quad \|\nabla \widehat{\mathcal{H}}(\mathbf{x}_{\Lambda^*}) - \nabla \widehat{\mathcal{H}}(\mathbf{x}_{\Lambda^*}^*)\|_2 = \|(\mathbf{A}_{\Lambda^*}^\top \mathbf{A}_{\Lambda^*} + 2\lambda(1-\gamma)\mathbf{I})(\mathbf{x}_{\Lambda^*} - \mathbf{x}_{\Lambda^*}^*)$$

$$\begin{aligned} &+ \lambda\gamma(\text{sign}(\mathbf{x}_{\Lambda^*}) - \text{sign}(\mathbf{x}_{\Lambda^*}^*)) + \lambda\gamma\alpha \left( \frac{\mathbf{x}_{\Lambda^*}}{\|\mathbf{x}_{\Lambda^*}\|_2} - \frac{\mathbf{x}_{\Lambda^*}^*}{\|\mathbf{x}_{\Lambda^*}^*\|_2} \right) \|_2 \\ &\stackrel{(a)}{\geq} \|(\mathbf{A}_{\Lambda^*}^\top \mathbf{A}_{\Lambda^*} + 2\lambda(1-\gamma)\mathbf{I})(\mathbf{x}_{\Lambda^*} - \mathbf{x}_{\Lambda^*}^*)\|_2 - \left\| \lambda\gamma\alpha \left( \frac{\mathbf{x}_{\Lambda^*}}{\|\mathbf{x}_{\Lambda^*}\|_2} - \frac{\mathbf{x}_{\Lambda^*}^*}{\|\mathbf{x}_{\Lambda^*}^*\|_2} \right) \right\|_2 \\ &\geq \|(\mathbf{A}_{\Lambda^*}^\top \mathbf{A}_{\Lambda^*} + 2\lambda(1-\gamma)\mathbf{I})(\mathbf{x}_{\Lambda^*} - \mathbf{x}_{\Lambda^*}^*)\|_2 - \lambda\gamma\alpha \cdot \frac{1}{\epsilon} \|\mathbf{x}_{\Lambda^*} - \mathbf{x}_{\Lambda^*}^*\|_2 \\ &\geq \left( \sigma_{\min}(\mathbf{A}_{\Lambda^*}^\top \mathbf{A}_{\Lambda^*} + 2\lambda(1-\gamma)\mathbf{I}) - \frac{\lambda\gamma\alpha}{\epsilon} \right) \|\mathbf{x}_{\Lambda^*} - \mathbf{x}_{\Lambda^*}^*\|_2. \end{aligned}$$

Letting  $\bar{\gamma} = \frac{\sigma_{\min}(\mathbf{A}_{\Lambda^*}^\top \mathbf{A}_{\Lambda^*}) + 2\lambda}{(\hat{L}\alpha + 2)\lambda}$ , then for  $\alpha \in (0, 1)$ ,  $\gamma \in (0, 1)$ , and  $\lambda > 0$ , one has  $\bar{\gamma} > 0$ . Put  $\tau = \sigma_{\min}(\mathbf{A}_{\Lambda^*}^\top \mathbf{A}_{\Lambda^*}) + 2\lambda(1-\gamma) - \frac{\lambda\gamma\alpha}{\epsilon}$  with  $0 < \gamma < \bar{\gamma} < 1$ . Then  $\tau > 0$  and

$$(4.16) \quad \|\nabla \widehat{\mathcal{H}}(\mathbf{x}_{\Lambda^*}) - \nabla \widehat{\mathcal{H}}(\mathbf{x}_{\Lambda^*}^*)\|_2 \geq \tau \|\mathbf{x}_{\Lambda^*} - \mathbf{x}_{\Lambda^*}^*\|_2.$$

Additionally, we show that  $\widehat{\mathcal{H}}$  is Lipschitz continuous on  $\Xi_{\Lambda^*} \cap B_\epsilon^c(\mathbf{0})_{\Lambda^*}$ . In fact, for any  $\mathbf{u}, \mathbf{v} \in \Xi_{\Lambda^*} \cap B_\epsilon^c(\mathbf{0})_{\Lambda^*}$ , we have

$$\begin{aligned} \|\nabla \widehat{\mathcal{H}}(\mathbf{u}) - \nabla \widehat{\mathcal{H}}(\mathbf{v})\|_2 &= \|(\mathbf{A}_{\Lambda^*}^\top \mathbf{A}_{\Lambda^*} + 2\lambda(1-\gamma)\mathbf{I})(\mathbf{u} - \mathbf{v}) + \lambda\gamma(\text{sign}(\mathbf{u}) - \text{sign}(\mathbf{v})) \\ &\quad + \lambda\gamma\alpha \left( \frac{\mathbf{u}}{\|\mathbf{u}\|_2} - \frac{\mathbf{v}}{\|\mathbf{v}\|_2} \right) \|_2 \\ &\leq \lambda\gamma\alpha \hat{L} \|\mathbf{u} - \mathbf{v}\|_2 + \|(\mathbf{A}_{\Lambda^*}^\top \mathbf{A}_{\Lambda^*} + 2\lambda(1-\gamma)\mathbf{I})(\mathbf{u} - \mathbf{v})\|_2 \leq L_{\widehat{\mathcal{H}}} \|\mathbf{u} - \mathbf{v}\|_2, \end{aligned}$$

where  $L_{\widehat{\mathcal{H}}} := \lambda\gamma\alpha\widehat{L} + \sigma_{\max}(\mathbf{A}_{\Lambda^*}^\top \mathbf{A}_{\Lambda^*}) + 2\lambda(1-\gamma)$ . Thus, for any  $\mathbf{x} \in \Xi \cap B_\epsilon^c(\mathbf{0})$ , one has  $\|\nabla \widehat{\mathcal{H}}(\mathbf{x}_{\Lambda^*}) - \nabla \widehat{\mathcal{H}}(\mathbf{x}_{\Lambda^*}^*)\|_2 \leq L_{\widehat{\mathcal{H}}} \|\mathbf{x}_{\Lambda^*} - \mathbf{x}_{\Lambda^*}^*\|_2$ . From the quadratic upper bound of  $\widehat{\mathcal{H}}$ , we obtain  $|\mathcal{H}(\mathbf{x}) - \mathcal{H}(\mathbf{x}^*)| \leq (\mathbf{x}_{\Lambda^*} - \mathbf{x}_{\Lambda^*}^*)^\top \nabla \widehat{\mathcal{H}}(\mathbf{x}_{\Lambda^*}) + \frac{L_{\widehat{\mathcal{H}}}}{2} \|\mathbf{x}_{\Lambda^*} - \mathbf{x}_{\Lambda^*}^*\|_2^2$ . Note that  $\mathbf{x}^*$  is a stationary point of  $\mathcal{H}$ , which implies  $\nabla \widehat{\mathcal{H}}(\mathbf{x}_{\Lambda^*}^*) = 0$ . Therefore, for any  $\mathbf{x} \in \Xi \cap B_\epsilon^c(\mathbf{0})$ , we have  $|\mathcal{H}(\mathbf{x}) - \mathcal{H}(\mathbf{x}^*)| \leq \frac{L_{\widehat{\mathcal{H}}}}{2} \|\mathbf{x}_{\Lambda^*} - \mathbf{x}_{\Lambda^*}^*\|_2^2$ . From inequality (4.16), we know that for any  $\mathbf{x} \in \Xi \cap B_\epsilon^c(\mathbf{0})$ ,  $|\mathcal{H}(\mathbf{x}) - \mathcal{H}(\mathbf{x}^*)| \leq \hbar \|\nabla \widehat{\mathcal{H}}(\mathbf{x}_{\Lambda^*})\|_2^2$ , where  $\hbar = L_{\widehat{\mathcal{H}}}/(2\tau^2)$ . Moreover, for  $\mathbf{x} \in \mathcal{X} := \{\mathbf{x} \in \mathbb{R}^n \mid \mathbf{x} \in \Xi \cap \mathcal{U}(\mathbf{x}^*) \text{ and } \zeta < \mathcal{H}(\mathbf{x}) < \zeta + \omega\}$ , where  $\mathcal{U}(\mathbf{x}^*)$  is a neighborhood of  $\mathbf{x}^*$  such that  $\mathcal{U}(\mathbf{x}^*) \subseteq B_\epsilon^c(\mathbf{0})$ , we have  $\text{dist}^2(0, \partial \mathcal{H}(\mathbf{x})) = \inf_{\xi \in \partial \mathcal{H}(\mathbf{x})} \|\xi\|_2^2 \geq \inf_{\xi \in \partial \mathcal{H}(\mathbf{x}^*)} \|\xi_{\Lambda^*}\|_2^2 = \|\nabla \widehat{\mathcal{H}}(\mathbf{x}_{\Lambda^*})\|_2^2 \geq |\mathcal{H}(\mathbf{x}) - \mathcal{H}(\mathbf{x}^*)|$  and so  $\mathcal{H}$  satisfies the KL property with exponent  $\frac{1}{2}$  on  $\Xi$ .

Finally, we prove the linear convergence rate of DCEN-DCA. Letting  $S_k = \sum_{i=k}^{\infty} \|\mathbf{x}_{i+1} - \mathbf{x}_i\|_2$ , then for any  $k \geq \tilde{K}$ , we have  $S_k = 2 \sum_{i=k}^{\infty} \frac{1}{2} \|\mathbf{x}_{i+1} - \mathbf{x}_i\|_2 \leq 2 \sum_{i=k}^{\infty} \left( \frac{L_h}{\mu_g} (\phi(\mathcal{H}(\mathbf{x}_{i-1}) - \zeta) - \phi(\mathcal{H}(\mathbf{x}_i) - \zeta)) \right) \leq \frac{2L_h}{\mu_g} \phi(\mathcal{H}(\mathbf{x}_{k-1}) - \zeta)$  and so  $S_k \leq \frac{2L_h}{\mu_g} \phi(\mathcal{H}(\mathbf{x}_{k-1}) - \zeta)$ . From the definition of the desingularizing function  $\phi$ , one has  $C(1-\theta)(\mathcal{H}(\mathbf{x}_{k-1}) - \zeta)^{-\theta} \text{dist}(0, \partial \mathcal{H}(\mathbf{x}_{k-1})) \geq 1$ . Since  $\|\mathbf{x}_k - \mathbf{x}_{k-1}\|_2 = S_{k-1} - S_k$ , we know that  $(\mathcal{H}(\mathbf{x}_{k-1}) - \zeta)^\theta \leq CL_h(1-\theta)(S_{k-1} - S_k)$ . Let  $\phi(\mathcal{H}(\mathbf{x}_{k-1}) - \zeta) = C(\mathcal{H}(\mathbf{x}_{k-1}) - \zeta)^{1-\theta}$ . Then  $C(\mathcal{H}(\mathbf{x}_{k-1}) - \zeta)^{1-\theta} \leq C(CL_h(1-\theta)(S_{k-1} - S_k))^{\frac{1-\theta}{\theta}}$  and so  $S_k \leq \frac{2L_h}{\mu_g} \phi(\mathcal{H}(\mathbf{x}_{k-1}) - \zeta) \leq \frac{2L_h}{\mu_g} \cdot C(CL_h(1-\theta)(S_{k-1} - S_k))^{\frac{1-\theta}{\theta}}$ . Letting  $C_1 = \frac{2L_h}{\mu_g} \cdot C(CL_h(1-\theta))^{\frac{1-\theta}{\theta}}$ , then one has  $S_k \leq C_1(S_{k-1} - S_k)^{\frac{1-\theta}{\theta}}$ . Substituting  $\theta = \frac{1}{2}$  yields  $C_1 = \frac{L_h^2 C^2}{\mu_g}$  and  $S_k \leq \frac{C_1^2 L_h^2}{\mu_g} (S_{k-1} - S_k)$ . Rearranging terms gives  $S_k \leq \frac{C_1}{1+C_1} S_{k-1}$ . Thus, there exists a  $K_3 > \tilde{K}$  such that  $\|\mathbf{x}_k - \mathbf{x}^*\|_2 \leq \sum_{i=k}^{\infty} \|\mathbf{x}_{i+1} - \mathbf{x}_i\|_2 = S_k \leq \frac{C_1}{1+C_1} S_{k-1} \leq \left(\frac{C_1}{1+C_1}\right)^{k-K_3} S_{K_3}$  for any  $k > K_3$ , which establishes linear convergence.  $\square$

**5. ADMM for Solving DCEN.** In this section, we develop an ADMM for solving DCEN. To this end, we introduce an auxiliary variable  $\mathbf{z} \in \mathbb{R}^n$  and impose  $\mathbf{x} - \mathbf{z} = \mathbf{0}$ . The equivalent constrained problem reads

$$(5.1) \quad \min_{\mathbf{x}, \mathbf{z} \in \mathbb{R}^n} \frac{1}{2} \|\mathbf{Ax} - \mathbf{b}\|_2^2 + \lambda \left( \gamma(\|\mathbf{z}\|_1 - \alpha \|\mathbf{z}\|_2) + (1-\gamma) \|\mathbf{z}\|_2^2 \right), \text{ s.t. } \mathbf{x} - \mathbf{z} = \mathbf{0}.$$

Then the augmented Lagrangian function associated with (5.1) is given by

$$(5.2) \quad \mathcal{L}_\rho(\mathbf{x}, \mathbf{z}, \mathbf{y}) = \frac{1}{2} \|\mathbf{Ax} - \mathbf{b}\|_2^2 + \lambda r_\gamma(\mathbf{z}) + \mathbf{y}^\top (\mathbf{x} - \mathbf{z}) + \frac{\rho}{2} \|\mathbf{x} - \mathbf{z}\|_2^2,$$

where  $\mathbf{y}$  denotes the dual variable and  $\rho > 0$  is a penalty parameter. By introducing the scaled dual variable  $\mathbf{u} = \mathbf{y}/\rho$ , we obtain the following ADMM iteration scheme:

$$(5.3a) \quad \mathbf{x}_{k+1} = \arg \min_{\mathbf{x} \in \mathbb{R}^n} \frac{1}{2} \|\mathbf{Ax} - \mathbf{b}\|_2^2 + \frac{\rho}{2} \|\mathbf{x} - (\mathbf{z}_k - \mathbf{u}_k)\|_2^2,$$

$$(5.3b) \quad \mathbf{z}_{k+1} = \arg \min_{\mathbf{z} \in \mathbb{R}^n} \lambda r_\gamma(\mathbf{z}) + \frac{\rho}{2} \|\mathbf{z} - (\mathbf{x}_{k+1} + \mathbf{u}_k)\|_2^2,$$

$$(5.3c) \quad \mathbf{u}_{k+1} = \mathbf{u}_k + \mathbf{x}_{k+1} - \mathbf{z}_{k+1}.$$

The  $\mathbf{x}$ -subproblem (5.3a) is a quadratic program with the closed-form solution  $\mathbf{x}_{k+1} = (\mathbf{A}^\top \mathbf{A} + \rho \mathbf{I})^{-1} (\mathbf{A}^\top \mathbf{b} + \rho(\mathbf{z}_k - \mathbf{u}_k))$ . Using the SMW identity, the  $\mathbf{x}$ -update

**Algorithm 5.1** ADMM for minimizing DCEN.

---

**Require:**  $\mathbf{A}, \mathbf{b}$ ; parameters  $\varepsilon_{\text{abs}}, \varepsilon_{\text{rel}}, \lambda, \rho > 0$ ,  $\alpha, \gamma \in (0, 1)$ , and  $K$  (maximum iteration).

**Ensure:** The optimal solution  $\mathbf{x}^*$ .

```

1: Initialize  $\mathbf{x}_0 = \mathbf{z}_0 = \mathbf{u}_0$ 
2: Compute  $\eta \leftarrow 3\lambda(1 - \gamma) + \rho$ 
3: for  $k = 0$  to  $K - 1$  do
4:   if the stopping condition (4.5) is not met then
5:     Compute  $\tilde{\mathbf{b}}_k \leftarrow \mathbf{A}^\top \mathbf{b} + \rho(\mathbf{z}_k - \mathbf{u}_k)$ 
6:     Update  $\mathbf{x}_{k+1} \leftarrow \rho^{-1} \tilde{\mathbf{b}}_k - \rho^{-2} \mathbf{A}^\top (\mathbf{I} + \rho^{-1} \mathbf{A} \mathbf{A}^\top)^{-1} \mathbf{A} \tilde{\mathbf{b}}_k$ 
7:     Update  $\mathbf{z}_{k+1} \leftarrow \text{prox}_{\frac{\lambda}{\rho} r_\gamma}(\mathbf{x}_{k+1} + \mathbf{u}_k)$ 
8:     Update  $\mathbf{u}_{k+1} \leftarrow \mathbf{u}_k + \mathbf{x}_{k+1} - \mathbf{z}_{k+1}$ 
9:     Compute  $\varepsilon_{\text{pri}}^k, \varepsilon_{\text{dual}}^k$ , and  $\text{relerr}_k$  via (4.6)
10:   else
11:      $\mathbf{x}^* \leftarrow \mathbf{x}_k$  ; break loop
12:   end if
13: end for

```

---

can be rewritten as  $\mathbf{x}_{k+1} = \frac{1}{\rho} \tilde{\mathbf{b}}_k - \frac{1}{\rho^2} \mathbf{A}^\top \mathbf{M}^{-1}(\mathbf{A} \tilde{\mathbf{b}}_k)$ , where  $\tilde{\mathbf{b}}_k = \mathbf{A}^\top \mathbf{b} + \rho(\mathbf{z}_k - \mathbf{u}_k)$  and  $\mathbf{M} = \mathbf{A} \mathbf{A}^\top + \rho \mathbf{I} \in \mathbb{R}^{m \times m}$ . The  $\mathbf{z}$ -subproblem admits a closed-form proximal solution. Specifically, it is updated as  $\mathbf{z}_{k+1} = \text{prox}_{\lambda/\rho r_\gamma}(\mathbf{x}_{k+1} + \mathbf{u}_k)$ . We summarize the procedure in Algorithm 5.1. For more discussions on the convergence analysis of the algorithm, interested readers are referred to [30, 32].

**6. Numerical experiments.** In this section, we validate the effectiveness of the DCEN method through numerical experiments on sparse signal recovery, MRI image reconstruction, and high-dimensional variable selection. All computational experiments were carried out on a PC equipped with an Intel Core i9-12900H processor (2.50 GHz), and the simulation environment was implemented on the MATLAB R2025b platform. We compare the DCEN model with the state-of-the-art models and algorithms in sparse recovery, including  $\ell_1$ -ADMM,  $\ell_p$  ( $p = 1/2$ ), IRLS- $\ell_p$  ( $p = 1/2$ ),  $\ell_1/\ell_\infty$ -FISTA,  $\ell_1/\ell_\infty$ -ADMM,  $\ell_1 - \alpha \ell_2$ -ADMM,  $\ell_1 - \alpha \ell_2$ -IAADMM ( $\alpha$  is iteratively adjusted),  $\ell_1 - \alpha \ell_2$ -DCA, and  $\ell_1 - \alpha \ell_2$ -FBS, for noiseless and noisy cases in subsections 6.2 and 6.3, respectively.

**6.1. Parameter settings.** To comprehensively evaluate the performance of the algorithm, we consider two types of sensing matrices  $\mathbf{A} \in \mathbb{R}^{m \times n}$  that are widely used in the compressed sensing literature.

- **Oversampled Discrete Cosine Transform (DCT) Matrix:** Following the construction methods in [27, 30, 35, 40], the column vectors  $\mathbf{a}_j$  are defined as  $\mathbf{a}_j := 1/\sqrt{m} \cdot \cos(2\pi \mathbf{w} j / F)$ ,  $j = 1, \dots, n$ , where  $\mathbf{w} \in [0, 1]^m$  is a random vector uniformly distributed within the unit hypercube. The parameter  $F > 0$  controls the coherence of the matrix; a larger value of  $F$  implies a higher correlation between column vectors, thereby increasing the difficulty of the recovery problem.
- **Gaussian Matrix:** This class of matrices is generated by sampling from a multivariate normal distribution  $\mathcal{N}(0, \Sigma)$ . By the settings in [40], the elements of the covariance matrix  $\Sigma$  are given by  $\Sigma_{i,j} = \{(1-r) * \mathbf{I}(i = j) + r\}_{i,j}$ , where  $r \in (0, 1)$  is the correlation coefficient. A higher value of  $r$  indicates strong correlation among observations, which is typically regarded as a chal-

lenging scenario for sparse recovery.

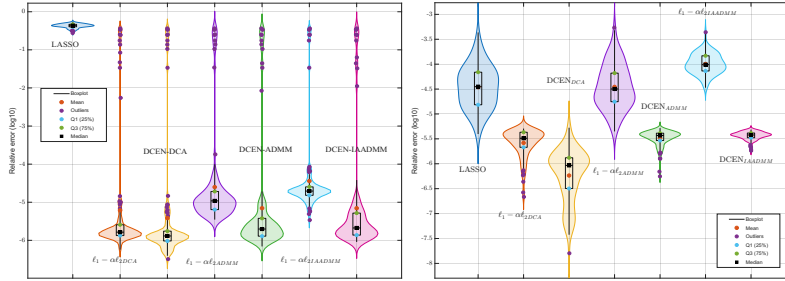
We set  $\epsilon = 10^{-6}$  and the maximum number of iterations  $K = 50$  for DCEN-DCA in Algorithm 4.1. For the DCEN-DCA subproblem in Algorithm 4.2 and Algorithm 5.1, we chose parameters  $\varepsilon_{\text{abs}} = 10^{-6}$ ,  $\varepsilon_{\text{rel}} = 10^{-6}$ ,  $\varepsilon = 10^{-6}$ , and the maximum number of iterations  $T = 5n$ . The parameter settings for DCA and ADMM, utilized for solving the  $\ell_1 - \alpha\ell_2$  model, are maintained consistent with those employed in DCEN. The same goes for  $\ell_1/\ell_\infty$ -ADMM. For  $\ell_1/\ell_\infty$ -FISTA, the algorithm is terminated once tolerance  $\text{tol} = 10^{-6}$  is satisfied or when the number of iterations reaches  $5n$ . All other settings of the algorithm were set to default ones. To obtain a high-quality initial estimate and avoid local minima, we adopt a warm-start strategy. Specifically, following the standard practice adopted in existing literature, we initialize all algorithms using the solution of  $\ell_1$ -ADMM [27, 30, 40]. We assess sparse recovery performance using the success rate, defined as the ratio of successful reconstructions to the total number of trials. A trial is considered successful when the relative error between the reconstruction vector  $\mathbf{x}^*$  and the ground truth signal  $\mathbf{x}^\sharp$  satisfies  $\frac{\|\mathbf{x}^* - \mathbf{x}^\sharp\|_2}{\|\mathbf{x}^\sharp\|_2} < 10^{-3}$ .

**6.2. Efficiency Evaluation in Noiseless Scenario.** This subsection is dedicated to comparing the efficiency of the DCEN model and its corresponding solver against established methods in a noiseless setting. The regularization parameters for all compared models are uniformly fixed at  $\lambda = 10^{-7}$ , with the exception of the  $\ell_p$  model, which employs an adaptive parameter selection strategy. Apart from the specific stopping criteria mentioned in Section 6.1, all remaining algorithmic parameters adopt their respective default settings.

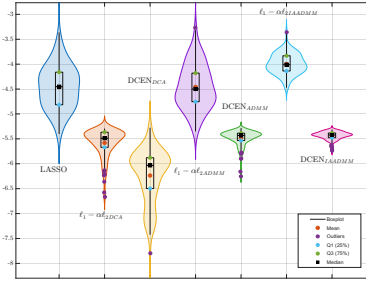
For the oversampled DCT matrix, the dimensions are set to  $300 \times 1000$ , with oversampling factors  $F = 20$  and  $F = 30$ , corresponding sparsity levels  $s = 10$  and  $s = 20$ , respectively, and a minimum separation between non-zero entries equal to  $F$ . For the Gaussian random matrix, the dimensions are set to  $64 \times 1024$ , with correlation parameters  $r = 0.2$  and  $r = 0.9$  corresponding to sparsity levels  $s = 10$  and  $s = 15$ , respectively. Each experimental configuration is repeated independently for 100 trials. Figure 2 compares the recovery accuracy of DCEN against the  $\ell_1 - \alpha\ell_2$  model across different sensing matrices and coherence levels, reporting the mean, median, and quantiles of the reconstruction error. The results demonstrate that DCEN consistently achieves superior recovery performance.

To enable a more systematic comparison, we unify the matrix dimensions to  $64 \times 1024$  for both the oversampled DCT and Gaussian random matrices. The oversampling factor  $F$  is set to 20 and 30, while the correlation parameter  $r$  for the Gaussian random matrix is set to 0.2 and 0.9. The sparsity level  $s$  is varied from 2 to 30 in increments of 2. Each configuration is again repeated 100 times. As shown in Figure 3(a), DCEN-DCA achieves significantly higher success rates than the  $\ell_1 - \alpha\ell_2$  model and other competing algorithms in high coherence scenarios. For Gaussian random matrices, the IRLS $\ell_p$  model exhibits excellent performance, consistent with the observations in [30] and [34]. Notably, both the IRLS $\ell_p$  and  $\ell_{1/2}$  models—solved via iteratively reweighted algorithms and half-thresholding, respectively—require prior knowledge of the true sparsity level  $s$  of the signal  $\mathbf{x}^\sharp$ . In our experiments, this ground-truth sparsity is provided. Leveraging this crucial prior information, the IRLS $\ell_p$  model attains substantially higher success rates compared to methods that do not assume sparsity knowledge.

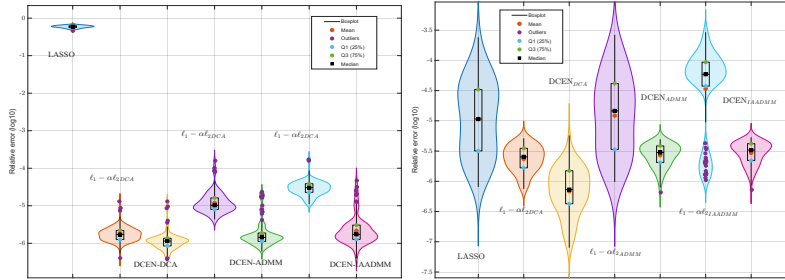
**6.3. Robust recovery of DCEN.** In this subsection, we evaluate the robust recovery performance of DCEN and its associated solvers—namely, the DCA and ADMM—in noisy scenarios. Specifically, contaminated measurements  $\mathbf{b}$  are generated



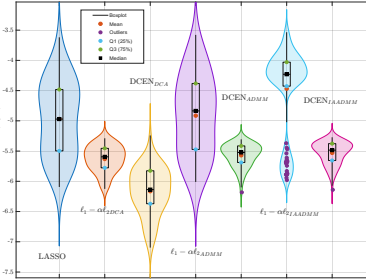
(a) Oversampled DCT matrix:  $F = 20$  and sparsity  $s = 20$ .



(b) Gaussian matrix:  $r = 0.2$  and sparsity  $s = 10$ .



(c) Oversampled DCT matrix:  $F = 30$  and sparsity  $s = 10$ .



(d) Gaussian matrix:  $r = 0.9$  and sparsity  $s = 15$ .

Fig. 2: Relative error distributions (log10) of LASSO,  $\ell_1 - \alpha\ell_2$ , and DCEN models under DCT/Gaussian sensing matrices with varying  $F$ ,  $r$ , and  $s$ .

Table 1: Reconstruction SNR (dB) for the DCEN and  $\ell_1 - \alpha\ell_2$  models and their solvers under varying noise levels using an oversampled DCT sensing matrix.

SNR(dB)	LASSO	$\ell_1 - \alpha\ell_2$ -DCA	DCEN-DCA	$\ell_1 - \alpha\ell_2$ -ADMM	DCEN-ADMM	$\ell_1 - \alpha\ell_2$ -IIADMM	DCEN-IIADMM
10dB	4.6616	6.5908	6.6227	6.5955	6.7078	6.6571	<b>6.7648</b>
20dB	10.9746	19.7750	<b>20.1652</b>	19.8222	19.9963	19.9177	20.1323
30dB	16.2115	28.6825	<b>28.7654</b>	28.6514	28.6351	28.6601	28.6668
40dB	27.1385	38.2164	38.3127	38.2961	38.2931	<b>38.4896</b>	38.4493
50dB	25.4694	37.0743	<b>37.1253</b>	37.0910	37.1123	37.0782	37.1143

by adding white Gaussian noise to the clean observation vector  $\mathbf{A}\mathbf{x}^\sharp$ , implemented in MATLAB via the `awgn` function. We consider five signal-to-noise ratio (SNR) levels: 10 dB, 20 dB, 30 dB, 40 dB, and 50 dB. For each noise level, we compute the reconstructed solution  $\mathbf{x}^*$  obtained from the  $\ell_1 - \ell_2$  and DCEN models and its algorithms, and evaluate the reconstruction SNR as  $10 \log_{10} \frac{\|\mathbf{x}^\sharp\|_2^2}{\|\mathbf{x}^* - \mathbf{x}^\sharp\|^2}$ .

Experiments are conducted on two types of sensing matrices. For the oversampled DCT matrix, we set its dimensions to  $100 \times 1000$ , with an oversampling factor  $F = 15$ , sparsity level  $s = 10$ , and a minimum separation of 15 between non-zero entries. For the Gaussian random matrix, the dimensions are also  $100 \times 1000$ , with a correlation parameter  $r = 0.9$  and sparsity level  $s = 30$ . Under each experimental configuration, we perform 50 independent trials and report the average reconstruction SNR across all runs. Table 1 presents the results for the oversampled DCT matrix. The regularization parameters  $\lambda$  and weight parameter  $\gamma$  are tuned according to the noise level using a

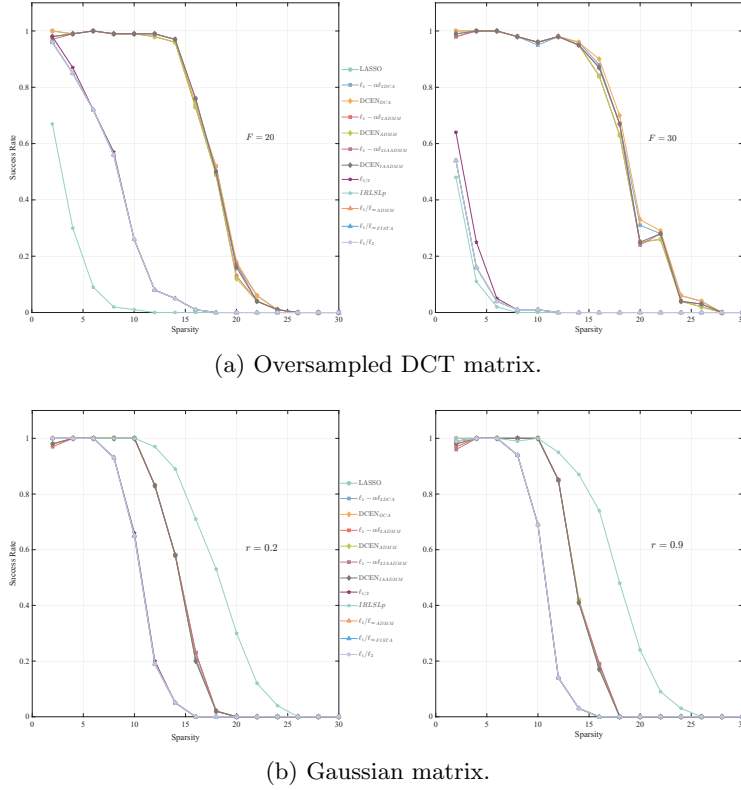


Fig. 3: Success rate versus sparsity  $s$  for oversampled DCT and Gaussian matrices.

Table 2: Reconstruction SNR (dB) for the DCEN and  $\ell_1 - \alpha\ell_2$  models and their solvers under varying noise levels using a high-coherence Gaussian random sensing matrix ( $r = 0.9$ ).

SNR(dB)	LASSO	$\ell_1 - \alpha\ell_2$ -DCA	DCEN-DCA	$\ell_1 - \alpha\ell_2$ -ADMM	DCEN-ADMM	$\ell_1 - \alpha\ell_2$ -IAADMM	DCEN-IAADMM
10dB	3.9467	5.1931	<b>5.2826</b>	5.2179	5.1183	5.2155	5.1155
20dB	3.8819	5.2219	<b>5.2695</b>	5.2362	5.1512	5.2299	5.1456
30dB	5.6162	8.3980	<b>8.5392</b>	8.3845	8.0089	8.3535	7.9788
40dB	5.7028	8.3714	<b>8.5469</b>	8.4014	8.1203	8.3869	8.1189
50dB	5.6703	8.7965	<b>8.8369</b>	8.8048	8.5151	8.7911	8.4710

grid search strategy. The results demonstrate that, in most cases, particularly when solved via DCA, DCEN achieves higher reconstruction SNR compared to the  $\ell_1 - \alpha\ell_2$  model. Table 2 reports the results for the Gaussian random matrix. Under high-coherence setting ( $r = 0.9$ ), DCEN-DCA exhibits a clear advantage, consistently outperforming both the  $\ell_1 - \alpha\ell_2$  model and ADMM-based variants. Notably, DCEN-DCA not only yields higher reconstruction accuracy but also demonstrates superior robustness across varying noise levels. In contrast, the performance of ADMM-type algorithms degrades, likely due to the adverse effects of high matrix coherence on convergence and algorithm parameters tuning. Overall, across all tested scenarios, DCEN-DCA consistently outperforms both ADMM-based solvers and the standard

$\ell_1$ - $\alpha\ell_2$  model.

**6.4. MRI Image Reconstruction.** In this subsection, we evaluate the performance of CDCEN for two-dimensional undersampled magnetic resonance imaging (MRI) reconstruction. Specifically, the DCEN-based reconstruction method is formulated as

$$(6.1) \quad \min_{\mathbf{u}} \gamma(\|\nabla \mathbf{u}\|_1 - \alpha\|\nabla \mathbf{u}\|_2) + (1 - \gamma)\|\nabla \mathbf{u}\|_2^2 \quad \text{s.t.} \quad \mathbf{R}\mathcal{F}\mathbf{u} = \mathbf{f},$$

where  $\mathcal{F}$  denotes the two-dimensional discrete Fourier transform,  $\mathbf{R}$  is a radial sampling mask in the frequency domain, and  $\mathbf{f}$  represents the observed  $k$ -space data. The objective function in (6.1) can be expressed as the difference of two convex functions; hence, it belongs to the class of DC programs. Consequently, the problem can be efficiently solved by combining DCA with the split Bregman method. At the  $k$ -th outer DCA iteration, the concave term  $-\|\nabla \mathbf{u}\|_2$  is linearized at the current iterate  $\mathbf{u}_k$ , yielding the convex subproblem

$$(6.2) \quad \min_{\mathbf{u}} \gamma(|\partial_{\mathbf{x}} \mathbf{u}| + |\partial_{\mathbf{y}} \mathbf{u}|) + (1 - \gamma)(|\partial_{\mathbf{x}} \mathbf{u}|^2 + |\partial_{\mathbf{y}} \mathbf{u}|^2) - \alpha\gamma\langle \mathbf{t}^k, \nabla \mathbf{u} \rangle \quad \text{s.t.} \quad \mathbf{R}\mathcal{F}\mathbf{u} = \mathbf{f},$$

where the gradient direction vector  $\mathbf{t}^k = (\mathbf{t}_{\mathbf{x}^k}, \mathbf{t}_{\mathbf{y}^k})$  is given by

$$(6.3) \quad \mathbf{t}^k = (\partial_{\mathbf{x}} \mathbf{u}^k, \partial_{\mathbf{y}} \mathbf{u}^k) / \sqrt{|\partial_{\mathbf{x}} \mathbf{u}^k|^2 + |\partial_{\mathbf{y}} \mathbf{u}^k|^2}.$$

To solve subproblem (6.2) efficiently, we introduce auxiliary variables  $\mathbf{d}_{\mathbf{x}} = \partial_{\mathbf{x}} \mathbf{u}$  and  $\mathbf{d}_{\mathbf{y}} = \partial_{\mathbf{y}} \mathbf{u}$ , and reformulate the problem (6.2) via quadratic penalization as

$$(6.4) \quad \begin{aligned} & (\mathbf{u}_{k+1}, \mathbf{d}_{\mathbf{x}_{k+1}}, \mathbf{d}_{\mathbf{y}_{k+1}}) \\ &= \arg \min_{\mathbf{u}, \mathbf{d}_{\mathbf{x}}, \mathbf{d}_{\mathbf{y}}} \gamma(|\mathbf{d}_{\mathbf{x}}| + |\mathbf{d}_{\mathbf{y}}|) + (1 - \gamma)(\mathbf{d}_{\mathbf{x}}^2 + \mathbf{d}_{\mathbf{y}}^2) - \gamma\alpha(\mathbf{t}_{\mathbf{x}}^k \mathbf{d}_{\mathbf{x}} + \mathbf{t}_{\mathbf{y}}^k \mathbf{d}_{\mathbf{y}}) \\ &+ \frac{\mu}{2} \|\mathbf{R}\mathcal{F}\mathbf{u} - \mathbf{f}\|_2^2 + \frac{\beta}{2} (\|\mathbf{d}_{\mathbf{x}} - \partial_{\mathbf{x}} \mathbf{u}\|_2^2 + \|\mathbf{d}_{\mathbf{y}} - \partial_{\mathbf{y}} \mathbf{u}\|_2^2). \end{aligned}$$

By introducing Bregman multipliers  $\mathbf{b} = (\mathbf{b}_{\mathbf{x}}, \mathbf{b}_{\mathbf{y}})$  for the constraint  $\mathbf{d} = \nabla \mathbf{u}$  and a dual variable  $\mathbf{z}$  for the data consistency constraint  $\mathbf{R}\mathcal{F}\mathbf{u} = \mathbf{f}$ , the split Bregman framework can be applied to solve (6.4) efficiently. The complete algorithmic procedure is summarized in Algorithm 6.1. Notably, when  $\gamma = 1$ , the model (6.1) reduces to the  $\ell_1 - \alpha\ell_2$  TV-type formulation, and the proposed algorithm simplifies to Algorithm 3 presented in [40].

We employ the standard Shepp-Logan phantom as the test image for our experiments. The comparative models include the classical TV- $\ell_1$ [5], MCTV- $\ell_1$  [23], TV- $\ell_2$ [29], MCTV- $\ell_2$ [29],  $\ell_1$ - $\ell_2$ , and  $\ell_1/\ell_2$  models. Figure 4 presents the reconstruction accuracy of all models under a radial sampling scheme with only eight projection lines. Experimental results demonstrate that DCEN-TV achieves the highest reconstruction accuracy. Compared to the  $\ell_1$ - $\ell_2$  model, the relative error of DCEN is reduced by an order of magnitude, indicating a significant improvement in reconstruction quality. Notably, although the  $\ell_1/\ell_2$  model is currently regarded as state-of-the-art in MRI reconstruction, it yields substantially higher relative errors than DCEN—highlighting the superior performance of our method in sparse MRI reconstruction.

**6.5. Variable Selection Performance under Highly Correlated Predictors.** To comprehensively evaluate the feature selection and sparse recovery performance of various sparse regression models in highly correlated scenarios, we conduct

---

**Algorithm 6.1** Split Bregman method for solving (6.1).

---

**Require:**  $\mathbf{R}, \mathbf{f}, \mathcal{F}$ ; parameters  $\mu, \beta > 0$ ;  $\gamma, \alpha \in (0, 1)$ ; maximum iterations **MAXOR** and **MAXIR**.

**Ensure:** Reconstructed image  $\mathbf{u}^*$ .

- 1: Initialize  $\mathbf{u} \leftarrow \mathbf{0}$ ,  $\mathbf{d}_x \leftarrow \mathbf{0}$ ,  $\mathbf{d}_y \leftarrow \mathbf{0}$ ,  $\mathbf{b}_x \leftarrow \mathbf{0}$ ,  $\mathbf{b}_y \leftarrow \mathbf{0}$ ,  $\mathbf{z} \leftarrow \mathbf{f}$
- 2: **for** outer = 1 to **MAXOR** **do**
- 3:   Update  $\mathbf{t}$  using (6.3)
- 4:   **for** inner = 1 to **MAXIR** **do**
- 5:      $\mathbf{u} \leftarrow (\mu \mathbf{R}^\top \mathbf{R} - \beta \mathcal{F} \Delta \mathcal{F}^\top)^{-1} (\mu \mathcal{F}^\top \mathbf{R} \mathbf{z} + \beta \mathbf{D}_x^\top (\mathbf{d}_x - \mathbf{b}_x) + \beta \mathbf{D}_y^\top (\mathbf{d}_y - \mathbf{b}_y))$
- 6:     Compute  $\mathbf{d}_x \leftarrow \text{shrink} \left( \frac{\gamma \alpha \mathbf{t}_x + \beta (\mathbf{D}_x \mathbf{u} + \mathbf{b}_x)}{\beta + 2(1 - \gamma)}, \frac{\gamma}{\beta + 2(1 - \gamma)} \right)$
- 7:     Compute  $\mathbf{d}_y \leftarrow \text{shrink} \left( \frac{\gamma \alpha \mathbf{t}_y + \beta (\mathbf{D}_y \mathbf{u} + \mathbf{b}_y)}{\beta + 2(1 - \gamma)}, \frac{\gamma}{\beta + 2(1 - \gamma)} \right)$
- 8:     Update  $\mathbf{b}_x \leftarrow \mathbf{b}_x + \mathbf{D}_x \mathbf{u} - \mathbf{d}_x$
- 9:     Update  $\mathbf{b}_y \leftarrow \mathbf{b}_y + \mathbf{D}_y \mathbf{u} - \mathbf{d}_y$
- 10:   **end for**
- 11:   Update  $\mathbf{z} \leftarrow \mathbf{z} + \mathbf{f} - \mathbf{R} \mathcal{F} \mathbf{u}$
- 12: **end for**
- 13:  $\mathbf{u}^* \leftarrow \mathbf{u}$

---

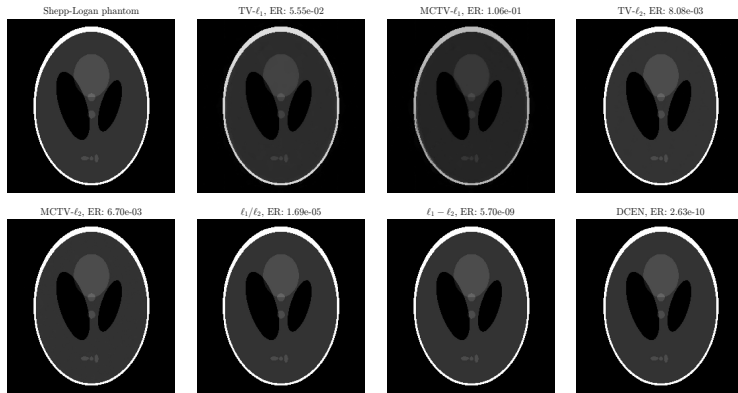


Fig. 4: MRI reconstruction results from 8 radial sampled projections.

the following numerical experiment. Specifically, the sample size is set to  $n = 20$  and the total number of variables is  $p = 100$ . The first three predictors are generated from a multivariate normal distribution  $\mathcal{N}(0, \Sigma)$  with covariance matrix  $\Sigma$  having off-diagonal entries  $\rho = 0.99$ , forming a highly correlated signal block. The remaining 97 predictors are i.i.d. standard normal noise. The true regression coefficients are nonzero only for the first three variables. Gaussian noise with standard deviation 1.2 is added to the response. All results are averaged over 100 independent Monte Carlo trials. We report the selection probabilities of the three true variables (Var1 to Var3), the average total number of selected variables, the average number of falsely selected noise variables, and the average selection rate of noise variables. The results are summarized in Table 3. Figure 5 reports the results obtained from 100 independent Monte Carlo simulations.

From Table 3, we know that LASSO and the  $\ell_1 - \alpha \ell_2$  penalty suffer from severely degraded selection probabilities under strong correlation (average true-variable re-

Table 3: Variable selection performance under highly correlated predictors. *Avg. total*: average number of selected variables; *Avg. false*: average number of falsely selected noise variables; *Noise sel. rate*: average per-noise-variable selection probability.

Method	Var1 $\uparrow$	Var2 $\uparrow$	Var3 $\uparrow$	Avg. total $\downarrow$	Avg. false $\downarrow$	Noise sel. rate $\downarrow$
LASSO	44.0%	16.0%	28.0%	6.48	5.60	5.77%
Elastic Net	78.0%	72.0%	78.0%	10.93	8.65	8.92%
$\ell_1 - \alpha\ell_2$	38.0%	11.0%	24.0%	3.07	2.34	2.41%
DCEN <sub>ADMM</sub>	85.0%	78.0%	86.0%	7.47	4.98	5.13%
DCEN <sub>DCA</sub>	60.0%	22.0%	49.0%	9.22	7.91	8.15%
$\ell_{1/2}$	87.0%	2.0%	19.0%	6.49	5.41	5.58%
$\ell_1/\ell_\infty$ FISTA	100.0%	0.0%	0.0%	8.53	7.53	7.76%
$\ell_1/\ell_2$	95.0%	21.0%	72.0%	24.06	22.18	22.87%

covery rates of only 29.3% and 24.3%, respectively). Elastic Net substantially improves the balance across correlated variables (average 76.0%), but at the cost of a markedly higher false discovery rate (8.65 noise variables on average). Several non-convex penalties (e.g.,  $\ell_1/\ell_\infty$  via FISTA and  $\ell_1/\ell_2$ ) exhibit extreme imbalance among correlated predictors, often concentrating nearly all nonzero mass on a single variable while discarding the others. DCEN-ADMM achieves the best overall trade-off: it attains true-variable selection probabilities of 85.0%, 78.0%, and 86.0% (average 83.0%, significantly superior to Elastic Net), while keeping the average number of falsely selected noise variables at only 4.98 and the noise selection rate at 5.13%. Compared with the DCA-based implementation of DCEN, ADMM demonstrates considerably greater stability in this highly challenging correlated regime. These findings indicate that DCEN-ADMM effectively mitigates the instability of traditional convex approaches and the tendency of purely nonconvex penalties to converge to poor local solutions. Consequently, it delivers substantially more reliable support recovery in the small-sample, high-dimensional, strongly correlated setting—a scenario of particular practical relevance in bioinformatics and imaging applications.

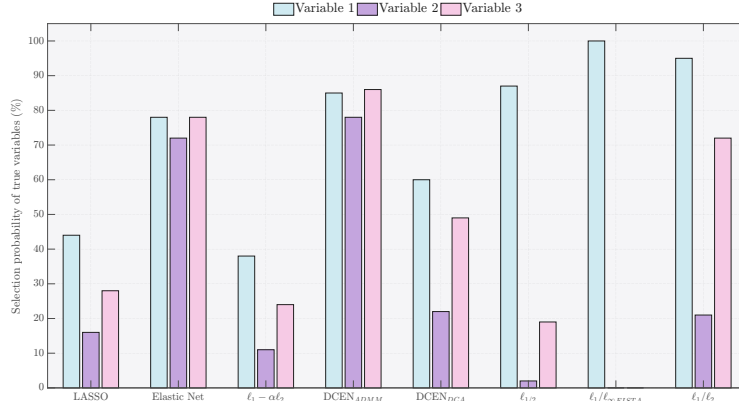


Fig. 5: Variable selection stability under highly correlated predictors ( $n = 20, p = 100$ ; averaged over 100 Monte Carlo trials).

**7. Conclusion.** This work proposes a unified DC modeling framework, termed DCEN, by integrating the nonconvex  $\ell_1 - \alpha\ell_2$  difference term with the convex  $\ell_2^2$  regularization. This formulation achieves an effective balance between strong sparsity promotion and solution stability, alleviating the bias of  $\ell_1$  regularization while

preserving robustness under highly correlated variables. With continuously tunable parameters, DCEN provides a unified modeling paradigm that encompasses and generalizes several representative models, including Lasso, Elastic Net, and the nonconvex  $\ell_1 - \alpha\ell_2$  model.

From a theoretical and algorithmic perspective, sufficient conditions for exact and stable recovery of DCEN are established under the RIP framework. Closed-form expressions of the proximal operator associated with the DCEN regularizer are derived, enabling the development of efficient optimization algorithms based on DCA and ADMM through DC decomposition and variable splitting. Moreover, within the KL analytical framework, the global convergence of DCA is rigorously proved, and its linear convergence rate is further characterized.

Furthermore, DCEN is extended to image processing applications by incorporating total variation regularization, leading to DCEN-TV, which is efficiently solved via a split Bregman method. Extensive numerical experiments on high-dimensional variable selection with strong correlations and MRI image reconstruction demonstrate that the proposed approach consistently outperforms state-of-the-art methods in terms of recovery accuracy, robustness, and noise resilience. Future work will focus on strengthening theoretical recovery guarantees, and extending DCEN to broader applications, including low-rank matrix recovery and multitask learning.

## REFERENCES

- [1] J. BOLTE, S. SABACH, AND M. TEBOULLE, *Proximal alternating linearized minimization for nonconvex and nonsmooth problems*, Math. Program., 146 (2014), pp. 459–494.
- [2] R. I. BOȚ, M. N. DAO, AND G. LI, *Extrapolated proximal subgradient algorithms for nonconvex and nonsmooth fractional programs*, Math. Oper. Res., 47 (2022), pp. 2415–2443.
- [3] S. BOYD, N. PARikh, E. CHU, B. PELEATO, J. ECKSTEIN, ET AL., *Distributed optimization and statistical learning via the alternating direction method of multipliers*, Found. Trends Mach. Learn., 3 (2011), pp. 1–122.
- [4] E. CANDES, M. RUDELSON, T. TAO, AND R. VERSHYNIN, *Error correction via linear programming*, in 46th Annual IEEE Symposium on Foundations of Computer Science (FOCS'05), IEEE, 2005, pp. 668–681.
- [5] E. J. CANDÈS, J. ROMBERG, AND T. TAO, *Robust uncertainty principles: Exact signal reconstruction from highly incomplete frequency information*, IEEE Trans. Inf. Theory, 52 (2006), pp. 489–509.
- [6] E. J. CANDÈS, M. B. WAKIN, AND S. P. BOYD, *Enhancing sparsity by reweighted  $\ell_1$  minimization*, J. Fourier Anal. Appl., 14 (2008), pp. 877–905.
- [7] R. CHARTRAND, *Exact reconstruction of sparse signals via nonconvex minimization*, IEEE Signal Process. Lett., 14 (2007), pp. 707–710.
- [8] S. S. CHEN, D. L. DONOHO, AND M. A. SAUNDERS, *Atomic decomposition by basis pursuit*, SIAM Rev., 43 (2001), pp. 129–159.
- [9] I. DAUBECHIES, R. DEVORE, M. FORNASIER, AND C. S. GÜNTÜRK, *Iteratively reweighted least squares minimization for sparse recovery*, Commun. Pure Appl. Math., 63 (2010), pp. 1–38.
- [10] D. L. DONOHO, *Compressed sensing*, IEEE Trans. Inf. Theory, 52 (2006), pp. 1289–1306.
- [11] E. ESSER, Y. LOU, AND J. XIN, *A method for finding structured sparse solutions to nonnegative least squares problems with applications*, SIAM J. Imaging Sci., 6 (2013), pp. 2010–2046.
- [12] J. FAN AND R. LI, *Variable selection via nonconcave penalized likelihood and its oracle properties*, J. Am. Stat. Assoc., 96 (2001), pp. 1348–1360.
- [13] A. FANNJIANG AND W. LIAO, *Coherence pattern-guided compressive sensing with unresolved grids*, SIAM J. Imaging Sci., 5 (2012), pp. 179–202.
- [14] H. GE AND P. LI, *The dantzig selector: recovery of signal via  $\ell_1 - \alpha\ell_2$  minimization*, Inverse Probl., 38 (2021), p. 015006.
- [15] F. GU AND A. WAN, *Nonconvex  $\ell_p - \alpha\ell_q$  minimization method and p-rip condition for stable recovery of approximately k-sparse signals*, Comput. Appl. Math., 43 (2024), p. 29.
- [16] P. O. HOYER, *Non-negative sparse coding*, in Proceedings of the 12th IEEE workshop on neural networks for signal processing, IEEE, 2002, pp. 557–565.
- [17] S. HUANG AND T. D. TRAN, *Sparse signal recovery via generalized entropy functions minimiza-*

*tion*, IEEE Trans. Signal Process., 67 (2018), pp. 1322–1337.

[18] L. HUO, W. CHEN, H. GE, AND M. K. NG,  $\ell_1 - \beta \ell_q$  minimization for signal and image recovery, SIAM J. Imaging Sci., 16 (2023), pp. 1886–1928.

[19] J. JIA, A. PRATER-BENNETTE, L. SHEN, AND E. E. TRIPP, Sparse recovery: The square of  $\ell_1/\ell_2$  norms, J. Sci. Comput., 102 (2025), p. 24.

[20] H. A. LE THI AND T. PHAM DINH, Dc programming and dca: thirty years of developments, Math. Program., 169 (2018), pp. 5–68.

[21] Q. LI, L. SHEN, N. ZHANG, AND J. ZHOU, A proximal algorithm with backtracked extrapolation for a class of structured fractional programming, Appl. Comput. Harmon. Anal., 56 (2022), pp. 98–122.

[22] T. LIU AND T. PONG, Further properties of the forward–backward envelope with applications to difference-of-convex programming, Comput. Optim. Appl., 67 (2017), pp. 489–520.

[23] Y. LIU, H. DU, Z. WANG, AND W. MEI, Convex mr brain image reconstruction via non-convex total variation minimization, Int. J. Imaging Syst. Technol., 28 (2018), pp. 246–253.

[24] Y. LOU AND M. YAN, Fast  $\ell_1 - \ell_2$  minimization via a proximal operator, J. Sci. Comput., 74 (2018), pp. 767–785.

[25] Y. LOU, P. YIN, Q. HE, AND J. XIN, Computing sparse representation in a highly coherent dictionary based on difference of  $\ell_1$  and  $\ell_2$ , J. Sci. Comput., 64 (2015), pp. 178–196.

[26] T. MA, Y. LOU, AND T. HUANG, Truncated  $\ell_{1-2}$  models for sparse recovery and rank minimization, SIAM J. Imaging Sci., 10 (2017), pp. 1346–1380.

[27] Y. RAHIMI, C. WANG, H. DONG, AND Y. LOU, A scale-invariant approach for sparse signal recovery, SIAM J. Sci. Comput., 41 (2019), pp. A3649–A3672.

[28] R. T. ROCKAFELLAR, *Convex Analysis*, Princeton University Press, Princeton, NJ, USA, 1970.

[29] M. SHEN, J. LI, T. ZHANG, AND J. ZOU, Magnetic resonance imaging reconstruction via non-convex total variation regularization, Int. J. Imaging Syst. Technol., 31 (2021), pp. 412–424.

[30] M. TAO, Minimization of  $\ell_1/\ell_2$  for sparse signal recovery with convergence guarantee, SIAM J. Sci. Comput., 44 (2022), pp. A770–A797.

[31] P. D. TAO AND L. T. H. AN, A dc optimization algorithm for solving the trust-region subproblem, SIAM J. Optim., 8 (1998), pp. 476–505.

[32] C. WANG, M. TAO, C. N. CHUAH, J. NAGY, AND Y. LOU, Minimizing  $\ell_1$  over  $\ell_2$  norms on the gradient, Inverse Probl., 38 (2022), p. 065011.

[33] C. WANG, M. TAO, J. G. NAGY, AND Y. LOU, Limited-angle ct reconstruction via the  $\ell_1/\ell_2$  minimization, SIAM J. Imaging Sci., 14 (2021), pp. 749–777.

[34] C. WANG, M. YAN, Y. RAHIMI, AND Y. LOU, Accelerated schemes for the  $\ell_1/\ell_2$  minimization, IEEE Trans. Signal Process., 68 (2020), pp. 2660–2669.

[35] J. WANG AND Q. MA, The variant of the iterative shrinkage-thresholding algorithm for minimization of the  $\ell_1$  over  $\ell_\infty$  norms, Signal Process., 211 (2023), p. 109104.

[36] Y. WANG, W. YIN, AND J. ZENG, Global convergence of admm in nonconvex nonsmooth optimization, J. Sci. Comput., 78 (2019), pp. 29–63.

[37] Y. XU, A. NARAYAN, H. TRAN, AND C. G. WEBSTER, Analysis of the ratio of  $\ell_1$  and  $\ell_2$  norms in compressed sensing, Appl. Comput. Harmon. Anal., 55 (2021), pp. 486–511.

[38] Z. XU, X. CHANG, F. XU, AND H. ZHANG,  $\ell_{1/2}$  regularization: A thresholding representation theory and a fast solver, IEEE Trans. Neural Netw. Learn. Syst., 23 (2012), pp. 1013–1027.

[39] L. YAN, Y. SHIN, AND D. XIU, Sparse approximation using  $\ell_1 - \ell_2$  minimization and its application to stochastic collocation, SIAM J. Sci. Comput., 39 (2017), pp. A229–A254.

[40] P. YIN, Y. LOU, Q. HE, AND J. XIN, Minimization of  $\ell_{1-2}$  for compressed sensing, SIAM J. Sci. Comput., 37 (2015), pp. A536–A563.

[41] L. ZENG, P. YU, AND T. K. PONG, Analysis and algorithms for some compressed sensing models based on  $\ell_1/\ell_2$  minimization, SIAM J. Optim., 31 (2021), pp. 1576–1603.

[42] K. ZHAN AND A. WAN, Sparse representation for  $\ell_p - \alpha \ell_q$  minimization and uniform condition for the recovery of approximately  $k$ -sparse signals with prior support information, Signal Process., 235 (2025), p. 110019.

[43] C. ZHANG, Nearly unbiased variable selection under minimax concave penalty, Ann. Stat., 38 (2010), pp. 894–942.

[44] S. ZHANG AND J. XIN, Minimization of transformed  $\ell_1$  penalty: theory, difference of convex function algorithm, and robust application in compressed sensing, Math. Program., 169 (2018), pp. 307–336.

[45] T. ZHANG, Analysis of multi-stage convex relaxation for sparse regularization, J. Mach. Learn. Res., 11 (2010).

[46] Z. ZHOU, A unified framework for constructing nonconvex regularizations, IEEE Signal Process. Lett., 29 (2022), pp. 479–483.

[47] Z. ZHOU, Rip analysis for the weighted  $\ell_r - \ell_1$  minimization method, Signal Process., 202

(2023), p. 108754.

[48] Z. ZHOU, *Recovery analysis for the  $\ell_p/\ell_1$  minimization problem*, J. Inverse Ill-Posed Probl., 33 (2025), pp. 61–80.

[49] Z. ZHOU AND J. YU, *Minimization of the  $q$ -ratio sparsity with  $1 < q \leq \infty$  for signal recovery*, Signal Process., 189 (2021), p. 108250.

[50] H. ZOU AND T. HASTIE, *Regularization and variable selection via the elastic net*, J. R. Stat. Soc. Ser. B Stat. Methodol., 67 (2005), pp. 301–320.